Strong electron-photon coupling in a one-dimensional quantum dot chain: Rabi waves and Rabi wave packets

G. Ya. Slepyan,[1] Y. D. Yerchak,[1,*] A. Hoffmann,[2] and F. G. Bass[3]
[1]*Institute for Nuclear Problems, Belarus State University, Bobruiskaya 11, 220050 Minsk, Belarus*
[2]*Institut für Festkörperphysik, Technische Universität Berlin, Hardenbergstrasse 36, 10623 Berlin, Germany*
[3]*Department of Physics, Bar-Ilan University, 52900 Ramat-Gan, Israel*
(Received 15 July 2009; revised manuscript received 4 January 2010; published 22 February 2010)

We predict and theoretically investigate the new coherent effect of nonlinear quantum optics—spatial propagation of Rabi oscillations (Rabi waves) in one-dimensional quantum dot (QD) chain. QD chain is modeled by the set of two-level quantum systems with tunnel coupling between neighboring QDs. The space propagation of Rabi waves in the form of traveling waves and wave packets is considered. It is shown, that traveling Rabi waves are quantum states of QD chain dressed by radiation. The dispersion characteristics of traveling Rabi waves are investigated and their dependence on average number of photons in wave is demonstrated. The propagation of Rabi wave packets is accompanied by the transfer of the inversion and quantum correlations along the QD chain and by the transformation of quantum light statistics. The conditions of experimental observability are analyzed. The effect is potentially useful for quantum computing and quantum informatics.

DOI: 10.1103/PhysRevB.81.085115 PACS number(s): 32.80.Xx, 42.65.Sf, 71.10.Li, 71.36.+c

I. INTRODUCTION

Rabi oscillations are periodical transitions of a two-level quantum system between its stationary states under the action of an oscillatory driving field, see, e.g. Refs. 1 and 2. The phenomenon was theoretically predicted by Rabi on nuclear spins in radio-frequency magnetic field[3] and was first observed by Torrey.[4] Afterwards, Rabi oscillations were discovered in various physical systems, such as electromagnetically driven atoms[5] (including the case of Rydberg atomic states[6]), semiconductor quantum dots (QDs),[7] and different types of solid-state qubits (superconducting charge qubits based on Josephson junctions,[8–10] spin qubits,[11] semiconductor charge qubits[12]). In real physical systems the ideal picture of Rabi effect, given by the Jaynes-Cummings model[1] can be essentially modified by additional features, such as the time-domain modulation of the field-matter coupling constant,[13,14] the phonon-induced dephasing,[15,16] and the local-field effects.[17–19] New phenomena appear in Rabi oscillators with broken inversion symmetry[20] and in systems of two coupled Rabi oscillators.[21–27]

In spatially extensive samples with a large number of oscillators the propagation effects come into play. As a result, the mechanism responsible for Rabi oscillations causes also a number of nonstationary coherent optical phenomena, such as optical nutation, photon echo, self-induced transparency, etc.[28] In low-dimensional systems the propagation effects also take place. For example, the numerical modeling of the coherent intersubband Rabi oscillations in a sample comprising 80 AlGaAs/GaAs quantum wells[29] shows that the population dynamics depends on the quantum well position in the series. This result demonstrates strong radiative coupling between wells and, more generally, significant difference in the picture of Rabi effect for single and multiple oscillators. Another aspects of such a difference, namely, the effects of quantum interference and correlations between photons in multiatom fluorescence, are demonstrated in Refs. 30 and 31 (on the example of atomic chains in nanofibers). From practical point of view, the effect of Rabi oscillations is a key ingredient for realization of binary logic and optical control in quantum informatics and quantum computing.

The theoretical analysis of Rabi oscillations is highly diversified both in form and content. The common feature is the impossibility of consideration of electromagnetic field influence as a small perturbation. Different ways of description are used in the analysis of the model problem of Rabi oscillations in a single two-level atom.[1] One such a way, the probability amplitude method, consists in solving of the Schrödinger equation for wave function $|\Psi\rangle$, which is the superposition of various atom-photon states. The second one is the Heisenberg operator method which is based on the analysis of the photonic and atomic operators time evolution. And finally, the third way is the unitary time-evolution operator technique. As is demonstrated in Ref. 1, all these methods lead to identical solutions; the choice of the concrete one is determined by the convenience considerations.

Taking into account the quantum nature of the electromagnetic field has the special significance in the analysis of Rabi oscillations in complex systems. Two different cases can be marked out. The first one could be called quasiclassical.[28] In this case external field has classical nature. However, the true field is supposed to be concordant with the quantum motions of the particles. So, the field should contain the contribution of the induced polarization, which has a quantum nature. Another case is really quantum and takes into consideration the photon structure of the electromagnetic field.[1] During the process of energy-level transitions in the atom the photon structure of the field is also transformed, therefore the atom-photon dynamics should be considered self-consistently.

In this paper we build a theoretical model of a distributed structure of coupled two-level systems exposed to the quantum light. We predict a new physical effect: the spatial propagation of Rabi oscillations in the form of traveling waves and wave packets. The oscillations of the population between levels in the isolated two-level system may be con-

sidered as a manifestation of the energy exchange between the system and photon. The critical issue when modeling the strong electron-photon coupling in distributed quantum system [for example, in one-dimensional (1D) QD chains] is the particle movement (e.g., interdot electron tunneling) leading to the quasimomentum exchange between charge carriers and photons. The interplay of these exchange mechanisms plays crucial role in the formation of spatial-temporal dynamics of Rabi oscillations in the QD chain. This mechanism precisely specifies the appearance of propagation effect. Not surprisingly, the presence of tunneling in this case cannot be represented as a small perturbation of ideal Rabi dynamics given by the model of isolated two-level system. It has a significantly more complicated behavior which cannot be described by means of any type of perturbation technique. Thus, more rigorous approach is required for such analysis. It is a sufficiently complicated task and it will be presented in this paper.

There exist different ways of theoretical description of complex quantum systems strongly interacted with quantum light. Often in quantum optics an "all-matter" picture is employed, where the dynamics of electromagnetic field is integrated out, for example, in the optical Bloch equations.[32,33] In Refs. 34 and 35 the light-matter interaction is treated in an "all-light" picture (Lippmann-Schwinger equation approach). As the theoretical approach we use the *probability amplitude method*, generalized for the case of 1D chain.

The paper is organized as follows. In Sec. II, we develop a theoretical model describing the QD chain—quantum light interaction. We formulate a model Hamiltonian with the separate terms accounting for the tunnel interdot coupling and local-field interaction (Sec. II A). Later on, we exploit the Hamiltonian for the derivation of equations of motion, describing dynamical properties of the system (Secs. II B and II C). To make the paper self-contained, we present the realistic ranges of variation for key QD parameters, used as phenomenological ones in our formulation (Sec. II D). In Sec. III we consider the traveling Rabi waves (dispersion equations, eigenmode structure, dispersion curves properties). In Sec. IV we investigate the Rabi wave packets propagation. The general solution of equation of motion is derived in Sec. IV A. Section IV B presents the simple analytical approximation of Rabi wave packet and qualitative analysis of its spatial-temporal dynamics. Sections IV C and IV D contain numerical results for different cases of initial quantum statistics of light (coherent states, Fock qubit states, vacuum Rabi waves). In Sec. V we consider the Rabi waves in a classic light limit. In Sec. VI we analyze local-field effect in the QD chain and identify the conditions leading to the weak influence of the local fields on Rabi wave propagation. The space-time structure of electron-electron and electron-photon correlators is considered in Sec. VII. The main results of the work are formulated in Sec. VIII.

II. MODEL

A. Hamiltonian

Let the infinite periodical one-dimensional chain of identical QDs be aligned parallel to the x axis. Let $|a_p\rangle$ and $|b_p\rangle$ to be one-electron orbital wave functions on the pth QD in the excited and ground states, respectively (Fig. 1).

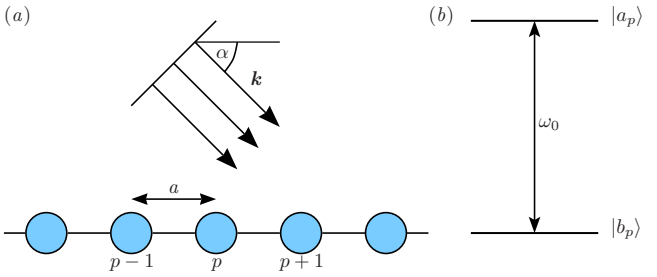

FIG. 1. (Color online) (a) Schematic picture of the QD chain interacting with single-mode electromagnetic field and (b) the energy levels diagram for pth QD.

Let the two neighboring QDs are coupled through the electron tunneling,[27] such that only intraband tunnel transitions are permitted. It means that the electron due to the electron tunneling can go from state $|a_p\rangle$ to state $|a_{p\pm1}\rangle$ and from state $|b_p\rangle$ to state $|b_{p\pm1}\rangle$ only. The transitions between ground and excited states of different QDs are assumed to be forbidden: $\langle a_{p\pm1}|b_p\rangle \approx 0$. In parallel with tunneling the interdot dipole-dipole interactions (such as Förster and the radiation field transfer) take place too. In given work we suppose the tunneling to be predominant mechanism of interdot coupling and neglect other ones. It will be shown below (see Sec. II D) that this assumption can be justified for a wide range of realistic parameter values.

Let the QD chain be exposed to a plane wave of quantum light, which is characterized by electric field operator given in the terms of creation and annihilation operators $\hat{a}^+$, $\hat{a}$ by $\hat{\boldsymbol{E}}(x)=\mathfrak{E}(\hat{a}e^{ikx}+\hat{a}^+e^{-ikx})$. Here, $\mathfrak{E}=\sqrt{2\pi\hbar\omega/V_0}\boldsymbol{e}$, V_0 is the normalizing volume, $\boldsymbol{e}$ is the unit polarization vector, $k=(\omega/c)\cos\alpha$ is the axial wave number, α and ω denote the angle of incidence and angular frequency, respectively [an $\exp(-i\omega t)$ time dependence is implicit].

The field dependence on transverse coordinates is negligibly small because of electrical QD smallness. The case of oblique incidence is of interest due to the possibility of axial wave number tuning with variation in incidence angle α at the constant frequency ω. Another case of basic importance is the interaction of the QD chain with strongly retarded surface wave (the waves of a such type propagate along the conductive carbon nanotubes,[36] interfaces between noble metal in the vicinity of plasmon resonance and dielectric media,[37] photonic crystal surfaces, etc).

In order to compare the theory of consideration and well-known basic (single-mode) theories, such as Jaynes-Cummings model[1] and Tavis-Cummings model,[38] we concentrate for simplicity on the single-mode approximation. The generalization for a multimode case thereafter being simple.

The Hamiltonian of the system in the rotating wave approximation[1] reads

$$\hat{H}=\hat{H}_d+\hat{H}_f+\hat{H}_{df}+\hat{H}_T+\Delta\hat{H}. \tag{1}$$

Here, $\hat{H}_d=(\hbar\omega_0/2)\Sigma_p\hat{\sigma}_{zp}$ corresponds to electron motion in the absence of electron tunneling and QD-field interaction,

$\hat{\sigma}_{zp}=|a_p\rangle\langle a_p|-|b_p\rangle\langle b_p|$, $\hat{H}_f=\hbar\omega\hat{a}^+\hat{a}$ is the Hamiltonian of the free electromagnetic field.[39] The component of the Hamiltonian

$$\hat{H}_{df}=\hbar g\sum_p(\hat{\sigma}_p^+\hat{a}e^{ikpa}+\hat{\sigma}_p^-\hat{a}^+e^{-ikpa}) \tag{2}$$

describes the QD-field interaction, where $g=-\boldsymbol{\mu}\mathcal{E}/\hbar$ is the interaction constant, $\boldsymbol{\mu}$ is the QD dipole moment. Let us assume that all transition dipole moments in the chain are characterized by real value and fixed orientation. The operator $\hat{\sigma}_p^+=|a_p\rangle\langle b_p|$ takes the pth QD in the ground state into the excited state, whereas operator $\hat{\sigma}_p^-=|b_p\rangle\langle a_p|$ takes the pth QD in the excited state into the ground state. The interdot electron tunneling can be described by the Hamiltonian

$$\hat{H}_T=-\hbar\xi_1\sum_p(|a_p\rangle\langle a_{p+1}|+|a_p\rangle\langle a_{p-1}|)-\hbar\xi_2\sum_p(|b_p\rangle\langle b_{p+1}|+|b_p\rangle\langle b_{p-1}|), \tag{3}$$

where $\xi_{1,2}$ are the electron tunneling frequencies for the excited (ξ_1) and ground (ξ_2) states of the QDs. The term $\Delta\hat{H}$ corresponds to the local-field effects originated from the dipole-dipole electron-hole (e-h) intradot interaction;[17–19] in the mean-field approximation this term is given by

$$\Delta\hat{H}=\frac{4\pi}{V}\boldsymbol{\mu}(\tilde{N}\boldsymbol{\mu})\sum_p(\hat{\sigma}_p^-\langle\hat{\sigma}_p^+\rangle+\hat{\sigma}_p^+\langle\hat{\sigma}_p^-\rangle). \tag{4}$$

Here, $\tilde{N}$ is the depolarization tensor [see Eq. (18) in Ref. 19] and V is the volume of the single QD.

In the model of consideration any relaxation mechanisms are omitted. The detailed analysis of the relaxation is not a subject of this paper. The simplest estimation of the relaxation influence can be done in the relaxation-time approximation (τ approximation). It needs a simple standard modification of final solutions obtained in the absence of relaxation (for more details see Secs. IV and V).

B. Equations of motion

The state vector of the "QD-chain+light" system may be represented in terms of the eigenstates of isolated QDs and photon number states as

$$|\Psi(t)\rangle=\sum_n\sum_p[A_{p,n}(t)|a_p,n\rangle+B_{p,n}(t)|b_p,n\rangle]. \tag{5}$$

Here, $|b_p,n\rangle=|b_p\rangle\otimes|n\rangle$ and $|a_p,n\rangle=|a_p\rangle\otimes|n\rangle$, where $|n\rangle$ is the light Fock state with n photons, $B_{p,n}$ and $A_{p,n}$ are the unknown probability amplitudes. It should be noted that if one omits last two terms in Hamiltonian (1), it goes into well-known Tavis-Cummings Hamiltonian.[38] However, the effect of superradiance, which is described by Tavis-Cummings model, is omitted in our analysis since we consider only the single-particle e-h states given by wave function Eq. (5).

The evolution of the system in the interaction picture is described by the nonstationary Schrödinger equation $i\hbar\partial_t|\Psi\rangle=\hat{V}|\Psi\rangle$, where the interaction Hamiltonian is given by $\hat{V}=\exp(i\hat{H}_ft/\hbar)(\hat{H}_d+\hat{H}_{df}+\hat{H}_T+\Delta\hat{H})\exp(-i\hat{H}_ft/\hbar)$. This Schrödinger equation leads to the following equations for the probability amplitudes:

$$\frac{\partial A_{p,n}}{\partial t}=-\frac{i\omega_0}{2}A_{p,n}+i\xi_1(A_{p-1,n}+A_{p+1,n})-ig\sqrt{n+1}B_{p,n+1}e^{i(kpa-\omega t)}-i\Delta\omega B_{p,n}\sum_m A_{p,m}B_{p,m}^*, \tag{6}$$

$$\frac{\partial B_{p,n+1}}{\partial t}=\frac{i\omega_0}{2}B_{p,n+1}+i\xi_2(B_{p-1,n+1}+B_{p+1,n+1})-ig\sqrt{n+1}A_{p,n}e^{-i(kpa-\omega t)}-i\Delta\omega A_{p,n+1}\sum_m A_{p,m}^*B_{p,m}, \tag{7}$$

where

$$\Delta\omega=\frac{4\pi}{\hbar V}\boldsymbol{\mu}(\tilde{N}\boldsymbol{\mu}) \tag{8}$$

is the local-field induced depolarization shift.[19] Obtaining this equations we have taken into account that the interaction Eq. (2) can cause the transitions between the states $|a_p,n\rangle$ and $|b_p,n+1\rangle$ only. As it is seen from Eqs. (6) and (7), two competitive mechanisms manifest themselves additionally to the ordinary Jaynes-Cummings dynamics: the local-field induced nonlinearity and quantum diffusion due to the interdot tunneling.

Let us restrict our consideration to the linear regime of the carrier motion and omit the terms $O(\Delta\omega)$ in Eqs. (6) and (7). By this means, we arrive at the set of coupled differential equations with respect to unknown vectors $\boldsymbol{\Psi}_{p,n}(t)=\begin{bmatrix}A_{p,n}(t)\\B_{p,n+1}(t)\end{bmatrix}$ as follows:

$$\partial_t\boldsymbol{\Psi}_{p,n}=\left[-\frac{i\omega_0}{2}\hat{\sigma}_z-ig\sqrt{n+1}\hat{\kappa}_p(t)\right]\boldsymbol{\Psi}_{p,n}+i\hat{\xi}(\boldsymbol{\Psi}_{p-1,n}+\boldsymbol{\Psi}_{p+1,n}), \tag{9}$$

where $\hat{\kappa}_p(t)=\hat{\sigma}_x\exp[i(\omega t-kpa)\hat{\sigma}_z]$, $\hat{\xi}=[(\xi_1+\xi_2)\hat{I}+(\xi_1-\xi_2)\hat{\sigma}_z]/2$, $\hat{I}$ denotes two-dimensional unit operator. Coefficients in Eq. (9) are expressed in terms of Pauli matrices

$$\hat{\sigma}_x=\begin{pmatrix}0&1\\1&0\end{pmatrix},\hat{\sigma}_y=\begin{pmatrix}0&-i\\i&0\end{pmatrix},\hat{\sigma}_z=\begin{pmatrix}1&0\\0&-1\end{pmatrix}, \tag{10}$$

acting on vectors $\boldsymbol{\Psi}_{p,n}(t)$. In the Sec. VI we shall analyze the limitations imposed by the nonlinear terms neglecting.

C. Continuous limit

In some cases it is more convenient to replace the recurrent ordinary differential Eq. (9) by the system of partial differential equations. To do this we should turn to the continuous limit, making the standard substitutions (see, for example, Ref. 40) $pa\to x$, $\boldsymbol{\Psi}_{p,n}\to\boldsymbol{\Psi}_n(x)$, $\boldsymbol{\Psi}_{p-1,n}+\boldsymbol{\Psi}_{p+1,n}-2\boldsymbol{\Psi}_{p,n}\to a^2\partial_x^2\boldsymbol{\Psi}_n$, and $\hat{\kappa}_p\to\hat{\kappa}(x)$. Then the system Eq. (9) leads to

$$\partial_t \mathbf{\Psi}_n = \left[2i\hat{\xi} - \frac{i\omega_0}{2}\hat{\sigma}_z - ig\sqrt{n+1}\,\hat{\kappa}(\omega t - kx) \right] \mathbf{\Psi}_n + ia^2\hat{\xi}\partial_x^2 \mathbf{\Psi}_n. \tag{11}$$

Equation (11) represents the system of partial differential equations with the variable matrix coefficient $\hat{\kappa}=\hat{\kappa}(\omega t-kx)$. This is the basic system for most of our further calculations.

The initial conditions of different types to Eq. (11) are dictated by the prior short-pulse optical pumping. Strictly speaking, the excitation of Rabi waves is uniform pump-probe process, therefore pump pulse should be included in the equations of motion. The rigorous modeling of optical pumping is by itself sufficiently complicated task. Thus, we focus on QD-chain interaction with the probe field, determined by the Hamiltonian (2). Thereby, the pumping component of electric field is removed from Eq. (11), but its contribution into the quantum state formation may be taken into account by the *a priori* chosen initial conditions to Eq. (11). Such approach is justified because of (i) sufficiently slight dependence of probability amplitudes on the fine details of pumping pulse configuration and (ii) a slight temporal overlap of pump and probe fields. Generally, initial distribution of probability amplitudes due to the optical pumping is a nonstationary state of e-h pair in QD chain, i.e., coherent superposition of ground and exited states. The initial distributions of probability amplitudes are determined by intensity and spatial structure of pumping pulse. For example, spatially confined Ψ wave packet for e-h pair in QD chain can be formed as a result of the pumping by the strongly focused optical beam, while for the traveling Ψ wave formation the pumping by the optical plane wave seems to be suitable.

D. Typical values of model parameters

For obtaining physical characteristics of Rabi waves using Eq. (11), the tunneling frequencies ξ_1 and ξ_2 and coupling factor g must be known *a priori*. Thus, $\xi_{1,2}$ or g are phenomenological parameters in our formulation. Even for defectless chains $\xi_{1,2}$, g depend on different factors and can vary in a wide range. The rigorous theoretical calculation of $\xi_{1,2}$, g is by itself a sufficiently complicated task, the results being highly dependent on the assumptions. For a numerical results reported in this paper, we extracted the values of physical and geometrical parameters from different model estimations as well as from experimental data. The realistic ranges of variation for model parameters are presented in Table I. These parameters are borrowed from different sources and mainly relate to the InGaAS QDs.

The values of tunneling frequencies $\xi_{1,2}$ have been estimated by using both numerical quantum-mechanical calculations[44] and simple quasiclassical approximations.[27,43] If the potential barrier height is about transition energy $\hbar\omega_0$ the condition $\xi_1 \gg \xi_2$ is satisfied.[43] For the case of the transition between higher quantum states (analog of Rydberg atom) both of levels can be placed near the barrier edge and therefore the tunneling frequencies become comparable: $\xi_1 \sim \xi_2$.

The QD dipole moment can be estimated as $\mu \sim e\sqrt[3]{V}$ (where e is the electron charge). Then the values of Ω_R from Table I correspond to the field strength $\mathcal{E} \sim 10-10^4$ V/cm. Such a values of field strength can be easily achievable. The strong coupling regime is dictated by the condition Ω_R, $2g \gg \tau^{-1}$, while the condition Ω_R, $2g \sim \xi_1$ establishes the coupling factor values for the principal interplay of interdot tunneling and Rabi dynamics. As one can see from Table I, these conditions are achievable in an experiment too.

Let us now discuss the ranges of applicability of the used model with e-h tunneling as the main interdot coupling factor. The estimations of the Förster and dipole-dipole interactions role are presented in a number of works (see, for example, Refs. 21 and 49).

According to the formulation of the model in Sec. II A, the dipole-dipole QD interactions can be ignored. This assumption can be justified as follows. The Förster energy is about $\hbar\mu^2/a^3$. For $\mu \sim 60$ D, $a \sim 20$ nm the value 30 μeV is obtained,[21] in good agreement with experiment[21] (the value of the same order is measured for dipole-dipole interaction too). For the $a \sim 5$ nm the value of Förster energy $\sim$69 meV is calculated in Ref. 49. The energy of tunneling coupling ($\hbar\xi_{1,2}$) decreases with rise of a exponentially, whereas the energy of Förster and dipole-dipole interactions diminishes algebraically, as a^{-3}. For sufficiently large a the contribution of these interactions to the interdot coupling becomes comparable with the tunneling contribution. We found that assumption holds true for QD chains that are not too rarefied (i.e., a is sufficiently small). In the Table I the range of interdot distances a for which the tunneling plays role of a dominant factor of interdot coupling is presented for potential barrier height $\sim$1 eV. As a result, at given interdot distances the inequality $ka \ll 1$ is fulfilled if the plane electromagnetic wave is chosen as a working mode. The value $ka \sim 1$ is reachable too, but for the case of surface wave with large retardation ($k \gg \omega/c$).

TABLE I. Typical parameter values for QD chain interacting with electromagnetic field. Symbol * denotes references containing experimental data.

Parameter	Symbol	Value	Reference
Quantum transition frequency	ω_0	$\sim$1 eV	
QD size	$\sqrt[3]{V}$	4–20 nm	22,41*, 42*, and 43
Interdot separation	a	10–20 nm	22,42*, and 43
Electron tunneling frequency	ξ_1	1–4.5 meV	42*, 43,44
Hole tunneling frequency	ξ_2	$0<\xi_2<\xi_1$	
Rabi frequency for classical light	Ω_R	10^{-2}–5 meV	22,43,45
Coupling constant for quantum light	g	0.07–2.5 meV	19,41*
Relaxation time	τ	$10^{-11}-10^{-9}$ s	19,21*, 44,46*, and 47
Depolarization shift	$\Delta\omega$	0.1 meV	19,48

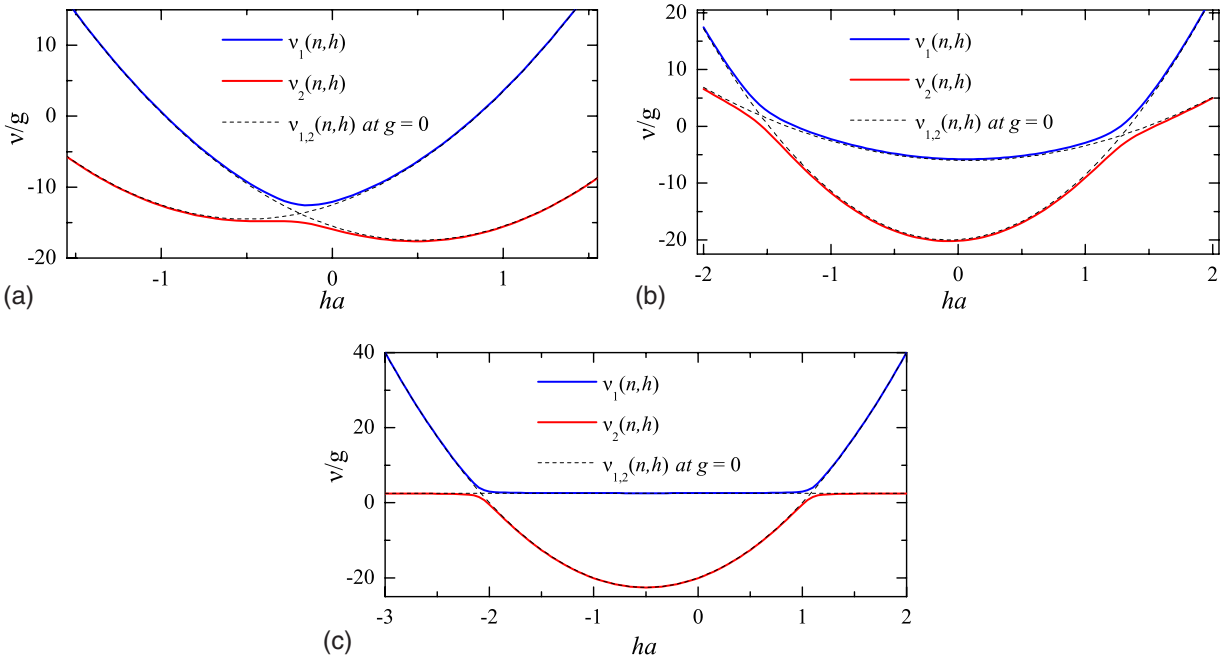

FIG. 2. (Color online) Dispersion curves for Rabi waves for different parameters values. The solid lines show results with electron-photon coupling, the dashed lines without it. (a) $\xi_1=\xi_2=8g$, $\Delta=3g$, $ka=1$, and $n=5$;(b) $\xi_1=10g$, $\xi_2=3g$, $\Delta=0$, $ka=0.143$, and $n=2$; (c) $\xi_1=10g$, $\xi_2=0$, $\Delta=-5g$, $ka=1$, and $n=5$.

III. TRAVELING RABI WAVES

A. Eigenmodes

Let us find the elementary solution of the system Eq. (11) in the form of traveling waves (hereafter referred to as Rabi waves): $A_n=u_n e^{i(h+k/2)x}e^{-i(\nu+\omega/2)t}$ and $B_{n+1}=v_{n+1}e^{i(h-k/2)x}e^{-i(\nu-\omega/2)t}$, where ν can now be identified as the unknown eigenfrequency for a given wave number h, u_n, and v_n are the sets of unknown constant coefficients. Substituting the chosen ansatz into Eq. (11) and omitting common factors, we obtain

$$\{\nu-\Delta/2+\vartheta_1(h)\}u_n-g\sqrt{n+1}v_{n+1}=0, \tag{12}$$

$$g\sqrt{n+1}u_n-\{\nu+\Delta/2+\vartheta_2(h)\}v_{n+1}=0, \tag{13}$$

where $\Delta=\omega_0-\omega$,

$$\vartheta_{1,2}(h)=\xi_{1,2}[2-a^2(h\pm k/2)^2]. \tag{14}$$

The existence of nontrivial solution of the system Eqs. (12) and (13) in respect to u_n and v_n requires that the respective determinant vanishes. It leads to a quadratic dispersion equation, which yields the values $\nu(h)$. Solving it with respect to ν, we determine the eigenfrequencies of system as

$$\nu_{1,2}(n,h)=-\frac{1}{2}[\vartheta_1(h)+\vartheta_2(h)\mp\Omega_n(h)]. \tag{15}$$

Here,

$$\Omega_n(h)=\sqrt{\Delta_{eff}^2+4g^2(n+1)}, \tag{16}$$

$$\Delta_{eff}(h)=\Delta-\vartheta_1(h)+\vartheta_2(h). \tag{17}$$

As it follows from Eq. (15), two different eigenmodes exist for each value of photon number n, namely,

$$|\Psi_{i,n}(t)\rangle=\sum_p[A_{i,n}(pa,t)|a_p,n\rangle+B_{i,n}(pa,t)|b_p,n+1\rangle], \tag{18}$$

where $i=1$, 2 is eigenmode number, the values $A_{i,n}(x,t)$ and $B_{i,n}(x,t)$ are defined by the expressions

$$A_{1,n}(x,t)=C_1e^{i(h+k/2)x}e^{-i(\nu_1+\omega/2)t},$$

$$B_{1,n+1}(x,t)=\frac{C_1g\sqrt{n+1}e^{i(h-k/2)x}e^{-i(\nu_1-\omega/2)t}}{\nu_1+\Delta/2+\vartheta_2}, \tag{19}$$

and

$$A_{2,n}(x,t)=\frac{C_2g\sqrt{n+1}e^{i(h+k/2)x}e^{-i(\nu_2+\omega/2)t}}{\nu_2-\Delta/2+\vartheta_2},$$

$$B_{2,n+1}(x,t)=C_2e^{i(h-k/2)x}e^{-i(\nu_2-\omega/2)t} \tag{20}$$

where $C_{1,2}\equiv C_{1,2}(n,h)$ are normalizing constants, the values $\vartheta_{1,2}\equiv\vartheta_{1,2}(h)$ and $\nu_{1,2}\equiv\nu_{1,2}(n,h)$ are expressed by the Eqs. (14) and (15), respectively.

B. Dispersion characteristics

Figure 2 exemplifies the dispersion characteristics of the two Rabi waves in a QD chain. Modes under examination are characterized by continuous spectrum (the value h varies continuously). The values $h>0$ correspond to the guided

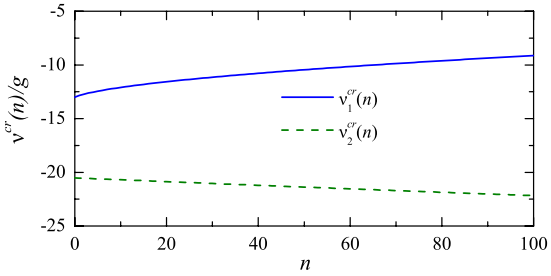

FIG. 3. (Color online) Dependence of critical frequencies of Rabi waves on the photon number, for the input parameters as follows: $\xi_1=10g$, $\xi_2=7g$, $\Delta=2(\xi_1-\xi_2)+\xi_2 a^2k^2$, and $ka=1$.

wave traveling in $+z$ direction, whereas the values $h<0$ correspond to the guided wave traveling in $-z$ direction. As Eqs. (12) and (13) for $k\neq 0$ are noninvariant with respect to the replacement $h\rightarrow -h$, wave propagation along $+z$ and $-z$ directions occurs nonanalogously. Therefore, *the reciprocity conditions break down*: $\nu_{1,2}(n,h)\neq\nu_{1,2}(n,-h)$. The reason is the existence of preferential direction, which is determined by the direction of photon mode propagation along the QD chain (sign of the value k).

For comparison, the dispersion curves are also shown when electron-photon coupling is ignored ($g=0$). One can note that in the limit $g\rightarrow 0$ both branches intersect. There is only one cross point for $\xi_1=\xi_2$, while there are two cross points in general case. In contrast, the cross points disappear for finite values g. Strictly speaking, because of electron-photon coupling the cross points shift from real h axis to the complex h plane.

The values $\nu_{1,2}$ are real for all real h. Therefore, the system being investigated is stable[50] with respect to the infinitely small perturbations. Dispersion equation for Eqs. (12) and (13) can be solved with respect to wave number $h(\nu)$ for given real-valued frequency ν. Thus, an analysis of dispersion laws yields for every mode the critical frequency $\nu_{1,2}^{cr}$ that for $\nu<\nu_{1,2}^{cr}$ the values $h_{1,2}(\nu)$ become complex. The critical frequencies are determined from the condition $\nu_{1,2}^{cr}(n)=\nu_{1,2}(n,h^{(0)})$, where the transcendental equation with respect to $h_{1,2}^{(0)}$ is as follows:

$$\left.\frac{\partial\nu_{1,2}(n,h)}{\partial h}\right|_{h=h_{1,2}^{(0)}}=0. \tag{21}$$

Physically, it means opacity of the QD chain for Rabi waves in the frequency regime below critical value.[50] At frequencies in the regime $\nu_2^{cr}<\nu<\nu_1^{cr}$ the QD chain is opaque only for one of the modes and at frequencies in the regime $\nu<\nu_{1,2}^{cr}$ it is nontransparent for both of them. One can choose the system parameters in such a way that at frequencies in the special regimes all real solutions $h(\nu)$ are either negative or positive [as an example see Fig. 2(a)]. This implies one-way opacity of the system, therefore Rabi waves could propagate in one direction only. The reason is the nonreciprocity of the system QD-chain+light.

It is significant, that critical values $\nu_{1,2}^{cr}$ for both modes depend on photon number n (see Fig. 3). This gives an important result, namely: *the conditions of transparency of the QD chain are different for Rabi waves with different photon numbers*. Note, that ν_1^{cr} increases and ν_2^{cr} decreases as n increases.

Usually both Rabi waves demonstrate the normal dispersion and propagate in the *same direction*. But for a special choice of parameters one of the two modes in the narrow frequency range indicates *anormalous dispersion*. For this mode phase and group velocities are oppositely directed [see Fig. 2(a)]. This behavior (along with nonreciprocal propagation) discriminate the Rabi waves with $k\neq 0$ from the Hopfield exciton polaritons in strong coupling regime (compare Figs. 2 and 4.23 in Ref. 51). The dispersion characteristics indicate special behavior for absolutely nontransparent ground-state barrier: $\xi_2=0$ [Fig. 2(c)]. In this case the group velocity $v_{gr}=\partial\nu/\partial h$ of one of the waves is very small for all h, except for the immediate vicinities of the cross points. As a result, the modes exchange their places passing through the cross points [e.g., on Fig. 2(c) $v_{gr}\approx 0$ for ν_1 mode between cross points $-2\lesssim ha\lesssim 1$ and for ν_2 mode at all other values of h]. Thus, except in the narrow ranges of wave number h, only one of the modes transfers the energy along the QD chain.

C. Discussion

Equation (11) in the limit of $g\rightarrow 0$ describes the electron-hole pairs in QD chain in equilibrium and inverse states, respectively. The probability amplitudes Eqs. (19) and (20) cease to depend on n and have the form

$$A_1(x,t)=C_1e^{iq_1x}e^{-i\omega_1(q_1)t}, \tag{22}$$

$$B_2(x,t)=C_2e^{iq_2x}e^{-i\omega_2(q_2)t}, \tag{23}$$

where $\omega_{1,2}(q)=\pm\omega_0/2-\xi_{1,2}(2-q^2a^2)$ and $A_2(x,t)=B_1(x,t)=0$. Electron-photon interaction (at $g\neq 0$) is responsible to the quantum transitions between the states in Eqs. (22) and (23) in the chain. In the strong coupling case these transitions take place in the regime of Rabi oscillations, i.e., they can be interpreted as a periodical chain of photon emissions absorptions and e-h pair creations annihilations, respectively. Such a type of oscillations is typical for different cases of strong coupling of condensed matter with light. For example, it is analogous to the exciton-photon strong coupling in the Hopfield polaritons[51–54] with the e-h pair instead of a Wannier exciton. The dependence $\omega_{1,2}(q)$ indicates the presence of spatial dispersion in the both cases.

According to Eqs. (19) and (20), the optical transitions between the states in Eqs. (22) and (23) occur satisfying the quasimomentum conservation law, which is dictated by the selection rule $q_1+k=q_2$. Thus, in contrast to the Hopfield polaritons, these transitions are *indirect* at $k\neq 0$. This mechanism of quasimomentum exchange between e-h pair and photon is precisely responsible to the spatial propagation of Rabi oscillations.

On the other hand, Eq. (18) in combination with Eqs. (19) and (20) constitute a generalization of the dressed states derived originally for two-level atom.[2] It should be noted, that in contrast to the isolated QD or low particle electrically small QD ensemble, the dressing parameter for QD chain is

spatially temporally modulated. In other words, because of the distributed geometry of QD chain the dressing moves along the QD chain according to the traveling wave law $\exp[i(kx-\omega t)]$.

Thus, each of the eigenmodes in Eqs. (19) and (20) comprise traveling waves with *different* wave numbers $h \pm k/2$. As a result, the Rabi wave propagation occurs as guided by an effective periodically inhomogeneous medium with the refractive index formed by spatially oscillating (with period $2\pi/k$) electric field. Therefore, the diffraction appears in the system. In the limit $k \to 0$, the medium turns homogeneous and the diffraction effect vanishes. The excitations in Eqs. (19) and (20) in this case are similar to the Hopfield polaritons. Parenthetically, the spatial oscillations of the partial amplitudes are because of interdot coupling, therefore they vanish in the limit of $\xi_{1,2} \to 0$.

The modes in Eqs. (19) and (20) can be excited independently on each other by a proper choice of initial conditions. For this case the Rabi oscillations do not take place, i.e., inversion is constant in space and time. This situation is similar to case of stationary states in Jaynes-Cummings model.[55] Generally, both of modes for given h may be excited together, which corresponds to the Rabi oscillations regime (inversion undergoes time-domain oscillations).

Another interesting case consists in simultaneous excitation of modes in Eqs. (19) and (20) with the same frequency ν (in doing so the wave numbers h will be different). This case corresponds to the spatial Rabi oscillations, with constant in time, but spatially modulated inversion density (inversion per unit QD).

Analogously to the other coherent excitations in condensed matter, Rabi waves in Eqs. (19) and (20) introduce a new family of quasiparticles (we name them rabitons). One can apply to them the standard secondary quantization technique, whereby they form a convenient basis for solving of different types of quantum-optical problems.

Similarly to the effect of self-induced transparency, the Rabi wave propagation can be interpreted as the motion of a precessing pseudodipole.[28] However, the coherence mechanisms in these two cases are principally different: in the Rabi wave the coherence is settled by the dispersion law in Eq. (15) while in the case of the self-induced transparency it has a solitonic character.

Note, that the reflections of Rabi waves and their mutual transformations at the field inhomogeneities become possible. Thus one obtain a unique possibility to control the processes of the reflection and transmission of Rabi waves by varying the spatial structure of the light.

IV. RABI WAVE PACKETS

A. Electron-photon dynamics

Let us next find the general solution of the system Eq. (11). In order to solve it we first write the equations for slowly varying amplitudes $\mathbf{\Phi}_n(x,t) = e^{i(\omega_0 t - kx)\hat{\sigma}_z/2}\mathbf{\Psi}_n(x,t)$. It then follows from Eq. (11) that:

$$\partial_t \mathbf{\Phi}_n - i[(2 - a^2k^2/4)\hat{\xi} - g\sqrt{n+1}\hat{\chi}(t)]\mathbf{\Phi}_n + a^2k\hat{\sigma}_z\hat{\xi}\partial_x\mathbf{\Phi}_n - ia^2\hat{\xi}\partial_x^2\mathbf{\Phi}_n = 0, \tag{24}$$

where $\hat{\chi}(t) = \hat{\sigma}_x \exp(-i\hat{\sigma}_z\Delta t)$. Let us note that coefficients of last system does not include the QD position x. This system can be solved by using the Fourier transform with respect to x

$$\mathbf{\Phi}_n(x,t) = \int_{-\infty}^{\infty} \tilde{\mathbf{\Phi}}_n(h,t)e^{ihx}dh. \tag{25}$$

Substituting Eq. (25) into Eq. (24), we replace the partial differential equations by the system of ordinary differential equations

$$\frac{d}{dt}\tilde{\mathbf{\Phi}}_n = i[\hat{\vartheta} - g\sqrt{n+1}\hat{\chi}(t)]\tilde{\mathbf{\Phi}}_n, \tag{26}$$

where $\hat{\vartheta} = \hat{\vartheta}(h) = \{[\vartheta_1(h) + \vartheta_2(h)]\hat{I} + [\vartheta_1(h) - \vartheta_2(h)]\hat{\sigma}_z\}/2$. The system Eq. (26) can be easily integrated, the solution is given by

$$\tilde{\mathbf{\Phi}}_n(h,t) = \hat{\rho}_n(h,t)\tilde{\mathbf{\Phi}}_n(h,0), \tag{27}$$

where

$$\hat{\rho}_n(h,t) = e^{i[\vartheta_1(h)+\vartheta_2(h)]t}e^{i\hat{\sigma}_z\Delta t}e^{i[\boldsymbol{m}\hat{\boldsymbol{\sigma}}\Omega_n(h)]t}, \tag{28}$$

$\hat{\boldsymbol{\sigma}} = (\hat{\sigma}_x, \hat{\sigma}_y, \hat{\sigma}_z)$, $\boldsymbol{m}$ is the unit vector of the form $(-2g\sqrt{n+1}/\Omega_n, 0, \Delta_{eff}/\Omega_n)$. The operator expression (28) can be written in matrix form as follows:

$$\hat{\rho}_n(h,t) = \begin{bmatrix} \varphi_n^-(h,t)e^{i\delta_+(h)t} & \psi_n(h,t)e^{i\delta_+(h)t} \\ \psi_n(h,t)e^{i\delta_-(h)t} & \varphi_n^+(h,t)e^{i\delta_-(h)t} \end{bmatrix}. \tag{29}$$

In the foregoing equations

$$\varphi_n^{\pm}(h,t) = \cos\frac{\Omega_n(h)t}{2} \pm i\frac{\Delta_{eff}(h)}{\Omega_n(h)}\sin\frac{\Omega_n(h)t}{2}, \tag{30}$$

$$\psi_n(h,t) = -i\frac{2g\sqrt{n+1}}{\Omega_n(h)}\sin\frac{\Omega_n(h)t}{2}, \tag{31}$$

$$\delta_{\pm}(h) = \frac{1}{2}[\vartheta_1(h) + \vartheta_2(h) \pm \Delta], \tag{32}$$

$\Omega_n(h)$ and $\Delta_{eff}(h)$ are determined by Eqs. (16) and (17), correspondingly, and $\tilde{\mathbf{\Phi}}_n(h,0)$ to be obtained from the initial conditions by the inverse Fourier transform

$$\tilde{\mathbf{\Phi}}_n(h,0) = \frac{1}{2\pi}\int_{-\infty}^{\infty} e^{-i(h\hat{I}+\hat{\sigma}_z k/2)x}\mathbf{\Psi}_n(x,0)dx. \tag{33}$$

Thus, for the vector of probability amplitudes $\mathbf{\Psi}_n(x,t)$ we have the following expression:

$$\mathbf{\Psi}_n(x,t) = e^{i(kx-\omega t)\hat{\sigma}_z/2} \times \int_{-\infty}^{\infty} \hat{\rho}_n(h,t)\tilde{\mathbf{\Phi}}_n(h,0)e^{i\{hx+[\vartheta_1(h)+\vartheta_2(h)]t/2\}}dh. \tag{34}$$

The account of relaxation in the framework of τ approximation can be made to Eq. (34) after implementing the replacement $\exp(-i\omega t\hat{\sigma}_z/2) \to \exp(-i\omega t\hat{\sigma}_z/2)\exp(-\lambda t/2)$, where $\lambda = \tau^{-1}$ is relaxation factor. The value of λ can be taken

from experimental data (see. Table I and references therein). Naturally, τ approximation is very rough model and its applicability is limited only qualitative assessments. For example, electron-phonon interaction, especially for longitudinal acoustic phonons is nonlinear,[15] which shows that for this case τ approximation becomes invalid. The detailed investigation of relaxation processes is beyond the scope of this paper and will be the subject of the further work.

Expression (34) in combination with Eq. (33) is the outcome of this section. It allows one to calculate such observables as inversion, exciton-exciton, and exciton-photon correlators for different initial states of light and QDs.

B. Dispersionless approximation

Let us now analyze the propagation of Rabi waves for the case of spatially localized initial e-h state. The QD chain is supposed to be initially either in the ground state $[A_n(x,0)=0$ for all $n]$ or in the excited state $[B_n(x,0)=0$ for all $n]$ or in the coherent superposition of two referred states.

Let us characterize the spatial-temporal dynamics of Rabi oscillations by the spatial density of the inversion (the inversion per unit QD)

$$w(x,t) = a\sum_n [|A_n(x,t)|^2 - |B_{n+1}(x,t)|^2]. \tag{35}$$

Another important quantity is the integral inversion $\tilde{w}(t)$, which is related to the spatial density of inversion by the expression

$$\tilde{w}(t) = \frac{1}{a}\int_{-\infty}^{\infty} w(x,t)dx. \tag{36}$$

In order to present illustrative results let us stop on the simple analytical solution of Eq. (11) making use the dispersionless approximation. Let us approximate the initial spatial distributions by the Gaussian beams $C_{A,B}\exp[-(x-d_{A,B})^2/2\sigma_{A,B}^2]$, where $C_{A,B}$, $d_{A,B}$, and $\sigma_{A,B}$ are normalization constants, positions of the beams, and their widths, respectively (the indexes A and B refer to excited and ground states of the electron in the QD chain, respectively).

According to Eq. (33) we obtain for $\tilde{\mathbf{\Phi}}_n(h,0)=\left[\begin{smallmatrix} a_n(h) \\ b_{n+1}(h)\end{smallmatrix}\right]$

$$a_n(h) \sim c(n)e^{-(h+k/2)^2\sigma_A^2/2}e^{-id_A(h+k/2)}, \tag{37}$$

$$b_{n+1}(h) \sim c(n+1)e^{-(h-k/2)^2\sigma_B^2/2}e^{-id_B(h-k/2)}, \tag{38}$$

where $c(n)$ is an arbitrary photonic distribution. One can see from Eqs. (37) and (38) that the spatial spectrum of $\mathbf{\Psi}_n(x,0)$ is given by two Gaussian peaks with peak widths $1/\sigma_{B,A}$ and positions of the peak centers $h_{1,2}^{(0)}=\pm k/2$, respectively. If $\sigma_{B,A}$ are sufficiently large, the spatial spectrums are strongly localized to the points $h_{1,2}^{(0)}$ and the main contribution to the integration in Eq. (34) comes from the narrow vicinities of the localization points. Assume $\vartheta_i(h)\cong\vartheta_i(h_{1,2}^{(0)})+(\partial\vartheta_i/\partial h)|_{h=h_{1,2}^{(0)}}(h-h_{1,2}^{(0)})$ and $\hat{\rho}_n(h,t)\cong\hat{\rho}_n(h_{1,2}^{(0)},t)$ (the dispersion effects neglecting). Having made the approximation we can express the integral Eq. (34) analytically. It leads to

$$\begin{aligned} A_n(x,t) = e^{i(kx-\omega t)/2}e^{-\lambda t}\{&[A_n(x+v_2^+t,0)\zeta_2^- e^{-i\nu_2^+ t} + A_n(x \\ &+ v_2^-t,0)\zeta_2^+ e^{-i\nu_2^- t}]e^{-ikx/2} + [B_{n+1}(x+v_1^-t,0)\eta_1 e^{-i\nu_1^- t} \\ &- B_{n+1}(x+v_1^+t,0)\eta_1 e^{-i\nu_1^+ t}]e^{ikx/2}\}, \end{aligned} \tag{39}$$

$$\begin{aligned} B_{n+1}(x,t) = e^{-i(kx-\omega t)/2}e^{-\lambda t}\{&[A_n(x+v_2^-t,0)\eta_2 e^{-i\nu_2^- t} - A_n(x \\ &+ v_2^+t,0)\eta_2 e^{-i\nu_2^+ t}]e^{-ikx/2} + [B_{n+1}(x+v_1^+t,0)\zeta_1^+ e^{-i\nu_1^+ t} \\ &+ B_{n+1}(x+v_1^-t,0)\zeta_1^- e^{-i\nu_1^- t}]e^{ikx/2}\}. \end{aligned} \tag{40}$$

Here, the velocities $v_{1,2}^{\pm}$ are defined as

$$v_1^{\pm} = v^{\pm}(h_1^{(0)}) = -2\xi_1 a^2 k\zeta_1^{\mp}, \tag{41}$$

$$v_2^{\pm} = v^{\pm}(h_2^{(0)}) = 2\xi_2 a^2 k\zeta_2^{\pm}, \tag{42}$$

the frequencies $\nu_{1,2}^{\pm}=\nu_{1,2}(n,\pm k/2)$ can be found from Eq. (15) after implementing the replacement $h=\pm k/2$ therein. The values $\zeta_{1,2}^{\pm}$ and $\eta_{1,2}$ are introduced to denote the amplitude factors, respectively:

$$\zeta_{1,2}^{\pm} = \frac{\Omega_n(h_{1,2}^{(0)}) \pm \Delta_{eff}(h_{1,2}^{(0)})}{2\Omega_n(h_{1,2}^{(0)})}, \tag{43}$$

$$\eta_{1,2} = \frac{g\sqrt{n+1}}{\Omega_n(h_{1,2}^{(0)})}. \tag{44}$$

Generally, as is apparent from Eqs. (39) and (40), any probability amplitude in the Rabi wave packet *is made of four components*. Each of them represents the separate subpacket, which is characterized by the own velocity of movement $v_{1,2}^{\pm}$, partial amplitude factors $\zeta_{1,2}^{\pm}$ and $\eta_{1,2}$, and frequency shifts $\nu_{1,2}^{\pm}$. Two of them [first and second terms in expressions (39) and (40)] correspond to the excited initial state and two another [third and fourth terms in Eqs. (39) and (40)] correspond to the ground initial state. The velocities in Eqs. (41) and (42) coincide with the group velocities of traveling Rabi waves in Eqs. (19) and (20) for $h=\pm k/2$: one can elementary verify, that $v_1^{\pm}=\partial\nu_{1,2}/\partial h|_{h=k/2}=v_{1,2}^{gr}(k/2)$ and $v_2^{\pm}=\partial\nu_{1,2}/\partial h|_{h=-k/2}=v_{1,2}^{gr}(-k/2)$. It is essential that the velocities $v_{1,2}^{\pm}$ as well as the frequency shifts $\nu_{1,2}^{\pm}$ depend on the photon number n. It means that the spatial propagation of wave packet is accompanied by the change in quantum light statistics (for example, if we assume that the light is initially in the coherent state, Poisson photon distribution transforms with propagation to the sub-Poisson or super-Poisson one). Of course, the region of asymptotic solution in Eqs. (39) and (40) is limited by the appearance of diffraction spreading.

Under the some specific conditions the number of subpackets could decrease. Two mechanisms of such decrease are possible: the first one is the tending to zero the subpacket amplitude and the second one is the confluence of the subpackets because of velocities synchronism.

As is seen from Eqs. (41) and (42), if

$$\Delta_{eff}(h_{1,2}^{(0)}) = 0, \tag{45}$$

for one pair of the subpackets the velocity synchronism condition $v_{1,2}^{+}=v_{1,2}^{-}$ is fulfilled. Notice that Eq. (45) is similar to

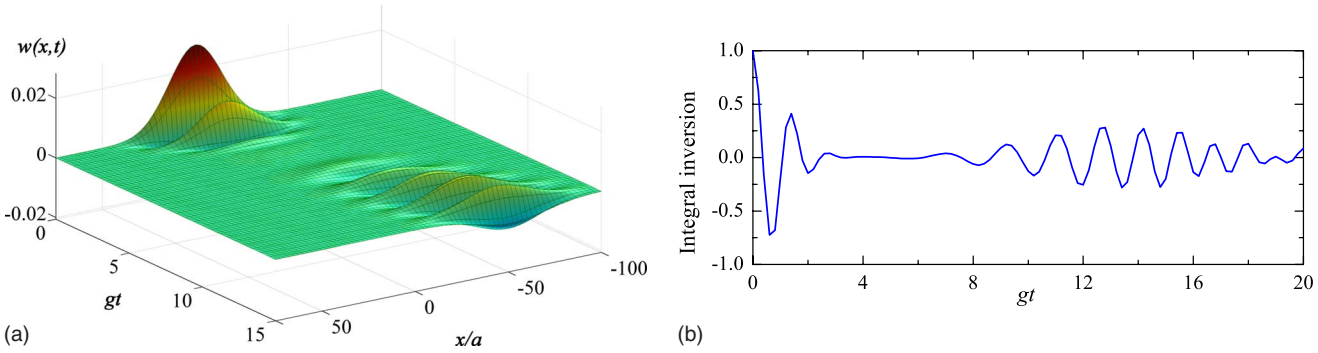

FIG. 4. (Color online) (a) Space-time distribution of the inversion density and (b) temporal dependence of the integral inversion in the QD chain for a coherent initial state of light ($\langle n\rangle=4$). The initial state of QD chain is a single Gaussian wave packet. $A_n(x,0)=c(n)\exp(-x^2/2\sigma^2)/\sqrt[4]{\pi\sigma^2}$, $B_{n+1}(x,0)=0$, $\xi_1=10g$, $\xi_2=7g$, $\Delta=2(\xi_1-\xi_2)+\xi_2 a^2k^2$, $ka=0.5$, $\sigma=20a$, and $\lambda=0.05g$.

the ordinary synchronism condition $\Delta=0$ in the single two-level system. The velocity synchronism condition for given QD-chain parameters can be fulfilled by fitting the value of the detuning Δ. If this is the case, three subpackets exist instead of four ones due to the confluence mechanism acting. Note, that $\Delta_{eff}(k/2)$ and $\Delta_{eff}(-k/2)$ cannot be equal to zero together at $k\neq 0$.

If the system is initially prepared in the stationary state, and the synchronism condition is fulfilled in the corresponding point [for example, $B_{n+1}(x,0)=0$ for any n and $\Delta_{eff}(-k/2)=0$], only one subpacket is preserved. In this case the expression for the inversion density becomes rather simple

$$w(x,t)=a\sum_n A_n^2(x+\xi_2 a^2 kt,0)[1-2\sin^2(g\sqrt{n+1}t)]. \tag{46}$$

The relaxation factor λ for simplicity is supposed to be zero. Expression (46) sums up contributions of different photonic states (terms with different n). Each contribution is the product of two multipliers describing different optical processes. The second multiplier represents the temporal law of Rabi oscillations with the frequencies $\nu_n=2g\sqrt{n+1}$, occurring in the isolated QD, while the first one indicates the movement of the region of Rabi oscillations along the QD chain with velocity $v=\xi_2 a^2 k$. One should note, that in the case of the exact synchronism v does not depend on n, whereby in this partial case the quantum statistics of light is not distorted with propagation of the wave packet. In particular, the initial coherence of quantum light persists in time. It is immediately follows from Eq. (36) and normalization condition that the integral inversion $\tilde{w}(t)$ associated to the inversion density Eq. (46) oscillates in time identically to the Rabi oscillations in the single two-level system [see Eq. (6.2.21) in Ref. 1 at $\Delta=0$].

The movement of the electron along the QD chain in the absence of electron-photon coupling is caused entirely by interdot tunneling through the corresponding energy level. As it shown in the remainder of this section, Rabi oscillations lead to a qualitatively new effects in the tunneling. According to Eqs. (39) and (40), the movement of the initially ground-state subpacket is governed by the tunneling transparency of the excited energy level and vice versa. This implies that the tunnel transition of the Rabi subpacket occur only through the opposite energy level after leaving the initial level due to the Rabi jump. If one of the barriers becomes absolutely opaque, the corresponding pair of subpackets does not move: $v_{1,2}^{\pm}\to 0$ at $\xi_{1,2}\to 0$. If inequality $\xi_1 \gg \xi_2$ is satisfied, the next surprising mechanism takes place: Rabi oscillations induce an abnormally high effective tunneling transparency for the initially ground-state subpacket as well as suppress it for initially excited one. Such a situation takes place even for $n=0$ [$B_n(x,0)=0$ for all n], whereby we conclude that the tunneling may be suppressed by the photon vacuum.

The existence of the momentum exchange between the photon and the e-h pair (see Sec. III C for more detail) is another necessary condition of Rabi subpackets motion: $v_{1,2}^{\pm}\to 0$ at $k\to 0$. The absence of such mechanism in Hopfield polaritons[51–54] makes above described effects impossible for them.

C. Coherent state: Collapses and revivals picture

Moving on to the more rigorous analysis of Rabi wave packets dynamics (in particular for taking into account the diffraction spreading) let us calculate the integrals in Eqs. (39) and (40) numerically. Consider the case of an excited initial state with space distribution in form of single Gaussian beam: $A_n(x,0)=c(n)\exp(-x^2/2\sigma^2)/\sqrt[4]{\pi\sigma^2}$ and $B_{n+1}(x,0)=0$. Assume that the light is initially prepared in the coherent state, so photon distribution is given by the Poisson law: $c(n)=\langle n\rangle^{n/2}e^{-\langle n\rangle/2}/\sqrt{n!}$, where $\langle n\rangle$ defines the average photon number. The spatial-temporal dynamics of inversion density for this case is depicted on Fig. 4(a). As is seen, an originally Gaussian packet temporally oscillates in agreement with ordinary trends of Rabi dynamics and, at the same time, moves along the chain. Oscillations collapse to zero quickly, but revive with time increasing *in another area of space*. The phenomenon of collapses and revivals of Rabi oscillations is well studied for isolated two-level system,[1,56] but the spacing between the collapse and subsequent revival is a manifestation of qualitatively new behavior, dictated by the interdot coupling. Long-time revivals in Jaynes-Cummings model have been predicted in Ref. 56 and interpreted as a quasicor-

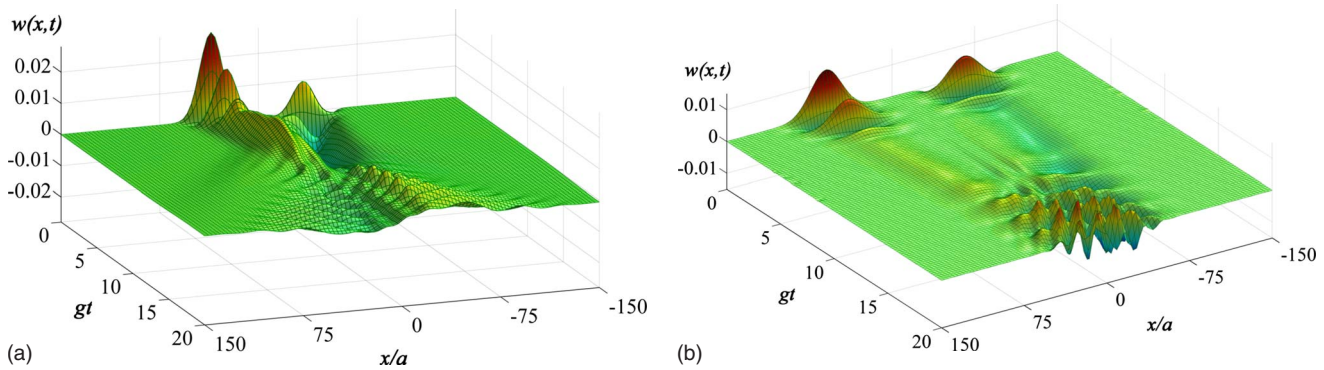

FIG. 5. (Color online) Space-time distribution of the inversion in the QD chain for the case of two counterpropagating wave packets. $A_n(x,0)=c(n)\exp[-(x-3\sigma)^2/2\sigma^2]/\sqrt[4]{4\pi\sigma^2}$ and $B_{n+1}(x,0)=c(n+1)\exp[-(x+3\sigma)^2/2\sigma^2]/\sqrt[4]{4\pi\sigma^2}$. The light is initially in coherent state ($\langle n\rangle=5$), $\Delta=0$, $\xi_1=\xi_2=10g$ and $ka=0.33$. (a) $\sigma=10a$ and $\lambda=0$ and (b) $\sigma=20a$ and $\lambda=0.05g$.

relations of initial coherence. The feature mentioned above means that in our model the spatial correlations exist as well as temporal ones. It will be demonstrated below by means of direct analysis of space-time correlators (see Sec. VII).

In spite of sufficiently low variations in the inversion density inside the packet [depicted in Fig. 4(a)], the integral inversion [presented in Fig. 4(b)] oscillates between −1 and 1, indicating strong light-QD coupling.

Let us examine now the case of initial QD state in the form of the coherent superposition [both $A_n(x,0)$ and $B_{n+1}(x,0)$ are nonzero]. As it has been noted above, the synchronism condition cannot be fulfilled together for both pair of subpackets (except the case of one of the pairs is motionless, see below). As a consequence, we have four subpackets in general case (or three ones if $\Delta_{eff}=0$ for one of the pairs). If $\xi_1=\xi_2=\xi$ (potential barriers with equal transparency) and $\Delta=0$, both pairs of packets move with pairwise equal velocities in opposite directions ($v_1^{\pm}=-v_2^{\pm}$). If the initial spatial distributions of probability amplitudes for ground and excited states are spaced ($d_A\neq d_B$), the subpackets will collide (see Fig. 5). Thus, initially Gaussian profiles of packets deform with time increasing due to the difference in subpacket velocities.

One should note that for the case of quantum external field in the coherent state QD chain cannot be saturated, i.e., the integral inversion cannot be a constant (see Fig. 6). The reason is the mutual asymmetry of $A_n(x,t)$ and $B_{n+1}(x,t)$ with respect to n and, as a result, $\Sigma_n\int_{-\infty}^{\infty}|A_n(x,t)|^2dx-\Sigma_n\int_{-\infty}^{\infty}|B_{n+1}(x,t)|^2dx$ is not a constant for any form of x dependence of $A_n(x,t)$ and $B_{n+1}(x,t)$. This asymmetry is caused entirely by quantum-field mechanisms and determines the contribution of QD interaction with photonic vacuum to the inversion. Therefore, it increases as the average photon number $\langle n\rangle$ decreases (compare Figs. 5 and 7).

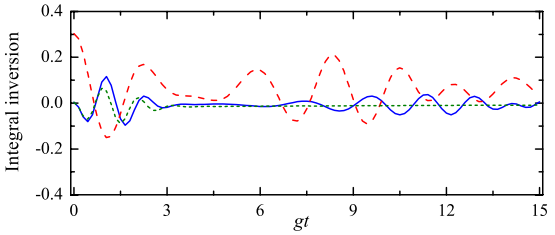

FIG. 6. (Color online) Temporal dependence of the integral inversion for a coherent initial state of light at the input parameters as follows: $\langle n\rangle=5$, $\sigma=20a$, and $\lambda=0.05g$ (solid line); $\langle n\rangle=5$, $\sigma=10a$, and $\lambda=0$ (dotted line); and $\langle n\rangle=0.5$, $\sigma=20a$, and $\lambda=0$ (dashed line). In all cases, $\xi_1=\xi_2=10g$, $\Delta=0$, and $ka=0.33$.

In another limiting case, for $\xi_2=0$ (fully opaque ground-state barrier), the velocities $v_2^{\pm}=0$ and one pair of subpackets do not moves along the chain. If, moreover, $\Delta_{eff}(k/2)=0$, then $v_1^{+}=v_1^{-}$, and the synchronism condition is fulfilled for both of packet pairs (see Fig. 8).

D. Fock qubit state and vacuum Rabi waves

Let us now consider the interaction of the QD chain with light in one more important initial state, namely, the Fock qubit state, i.e., a superposition of two Fock states: $|\psi_f(0)\rangle=C_1|N\rangle+C_2|N+1\rangle$, where N is an arbitrary fixed number, $C_{1,2}$ a given number, satisfying the normalization condition. As in the previous case, the initial spatial distributions of e-h pair probability amplitudes would be approximated by the Gaussian beams with spatial spectrums in Eqs. (37) and (38). The spatial-temporal dynamics of the inversion density for the initial state of field $|\psi_f(0)\rangle=1/\sqrt{2}|0\rangle+1/\sqrt{2}|1\rangle$ is shown

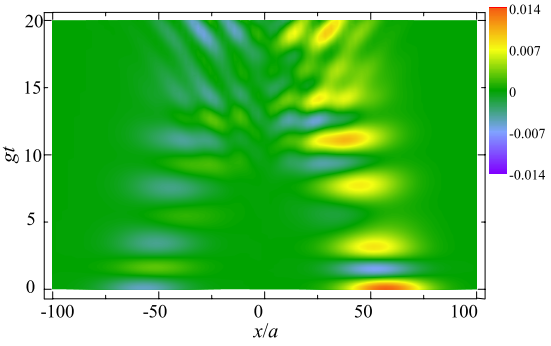

FIG. 7. (Color online) The asymmetry of the inversion space-time distribution for two counterpropagating wave packets in case of the coherent state of light with small average number of the photons $\langle n\rangle=0.5$. $A_n(x,0)=c(n)\exp[-(x-3\sigma)^2/2\sigma^2]/\sqrt[4]{4\pi\sigma^2}$, $B_{n+1}(x,0)=c(n+1)\exp[-(x+3\sigma)^2/2\sigma^2]/\sqrt[4]{4\pi\sigma^2}$, $\xi_1=\xi_2=10g$, $\Delta=0$, $ka=0.33$, $\sigma=20a$, and $\lambda=0$.

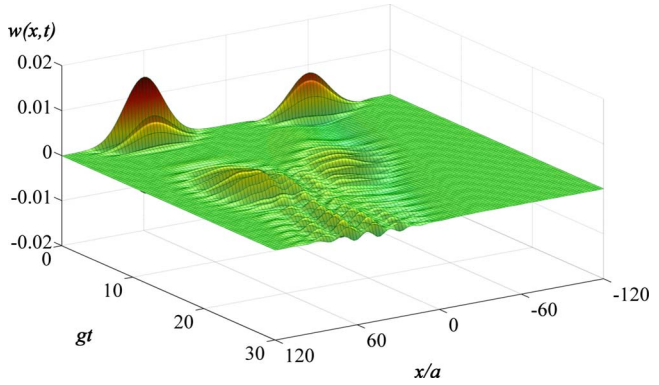

FIG. 8. (Color online) Space-time distribution of the inversion in the QD chain for the case of the fully opaque ground-state barrier. $A_n(x,0)=c(n)\exp[-(x-3\sigma)^2/2\sigma^2]/\sqrt[4]{4\pi\sigma^2}$, $B_{n+1}(x,0)=c(n+1)\exp[-(x+3\sigma)^2/2\sigma^2]/\sqrt[4]{4\pi\sigma^2}$, $\xi_1=10g$, $\xi_2=0$, $\Delta=2(\xi_1-\xi_2)-\xi_1 a^2k^2$, $ka=0.5$, $\sigma=20a$, and $\lambda=0.05g$. The light is initially in the coherent state with $\langle n\rangle=5$.

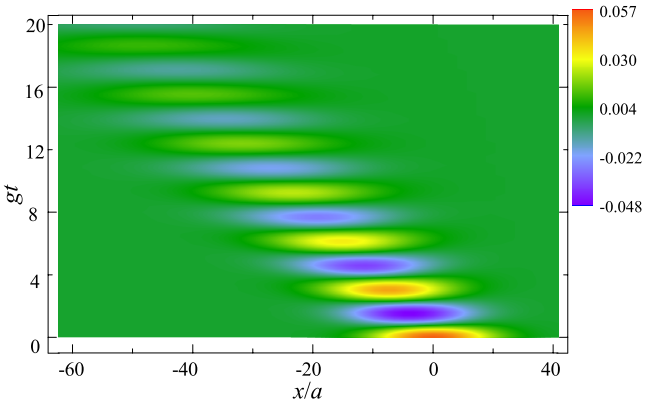

FIG. 10. (Color online) Space-time distribution of the inversion in the QD chain for the vacuum initial state of the field. $A_0(x,0)=(1/\sqrt[4]{\pi\sigma^2})\exp(-x^2/2\sigma^2)$ and $A_n(x,0)=0$ for $n\geq 1$ and $B_n(x,0)=0$ for all n, $\xi_1=6g$, $\xi_2=5g$, $\Delta=2(\xi_1-\xi_2)+\xi_2 a^2k^2$, $\sigma=10a$, $ka=0.5$, and $\lambda=0.05g$.

in Fig. 9(a). It can be seen from the figure, that Rabi wave packet does not collapses and revives, but oscillates in a complicated manner [see also integral inversion dynamics, Fig. 9(b)].

In the remainder of this section we consider the spatial propagation of vacuum Rabi oscillations. It is well known that such type of Rabi oscillations exist in initially excited two-level system strongly coupled with zero-photon light mode, as a result of spontaneous emission.[1] The similar effect takes place in the QD chain, but in contrast to uncoupled two-level systems, temporal oscillations accompanied by its spatial movement, which is illustrated by Fig. 10. The spontaneous emission support couples single-mode zero-photon state with one-photon state only, thus, this excitation can be imagined as a wave beam characterized by the monochromatic Rabi-frequency spectrum and continuous spatial spectrum at the same time. However, it should be noted that one need to use a multimode light theory for full treatment of condensed matter interaction with photonic vacuum.[39] This problem for Rabi waves is a subject for future considerations.

V. CLASSICAL LIGHT LIMIT

Let us move on to the quasiclassical limit of Rabi waves theory. Here, we focus only on the case when the incident electromagnetic field is prepared in the coherent state with the large average photonic number $\langle n\rangle$, thereby permitting us to neglect the quantum nature of the light and replace the electric field operator by its expectation value $\boldsymbol{E}(x,t)=\mathrm{Re}\{\mathfrak{E}\exp[i(kx-\omega t)]\}$. Omitting the local-field effects as before, we can write the simplified Hamiltonian of the system "QD-chain-electromagnetic field" in the form $\hat{H}=\hat{H}_0+\hat{H}_T$, where the term

$$\hat{H}_0=\frac{\hbar\omega_0}{2}\sum_n\hat{\sigma}_{zn}-\frac{\hbar\Omega_R}{2}\sum_n[\hat{\sigma}_n^+e^{i(nka-\omega t)}+\mathrm{H.c.}] \quad (47)$$

describes Rabi oscillations in noninteracting QDs and $\Omega_R=\boldsymbol{\mu}\mathfrak{E}/\hbar$ is the Rabi frequency.[1] The interdot interaction mechanism and light properties are independent of each other, so the term $\hat{H}_T$ is defined as before by Eq. (3).

The state vector of the system has the form of coherent superposition

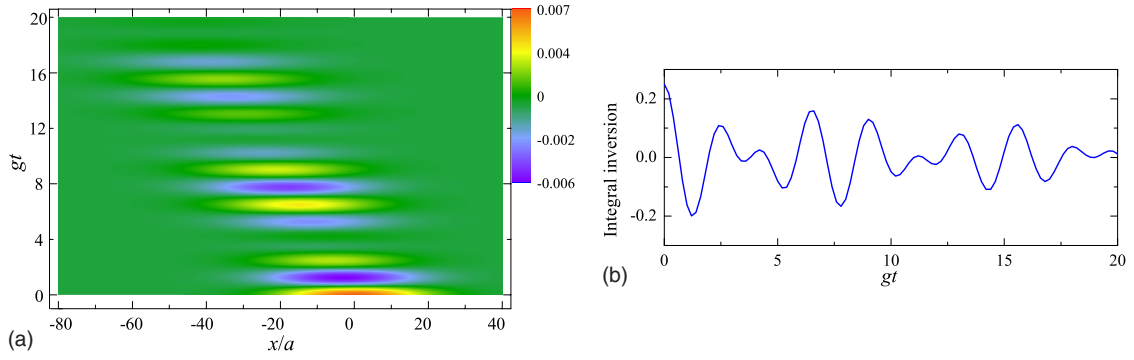

FIG. 9. (Color online) (a) Space-time distribution of the inversion and (b) temporal dependence of the integral inversion in the QD chain for the field in the Fock qubit initial state. $|\psi_f(0)\rangle=1/\sqrt{2}|0\rangle+1/\sqrt{2}|1\rangle$, $A_0(x,0)=A_1(x,0)=(1/\sqrt[4]{\pi\sigma^2})\exp(-x^2/2\sigma^2)$ and $A_n(x,0)=0$ for $n\geq 2$ and $B_n(x,0)=0$ for all n, $\xi_1=10g$, $\xi_2=7g$, $\Delta=2(\xi_1-\xi_2)+\xi_2 a^2k^2$, $\sigma=20a$, $ka=0.33$, and $\lambda=0.05g$.

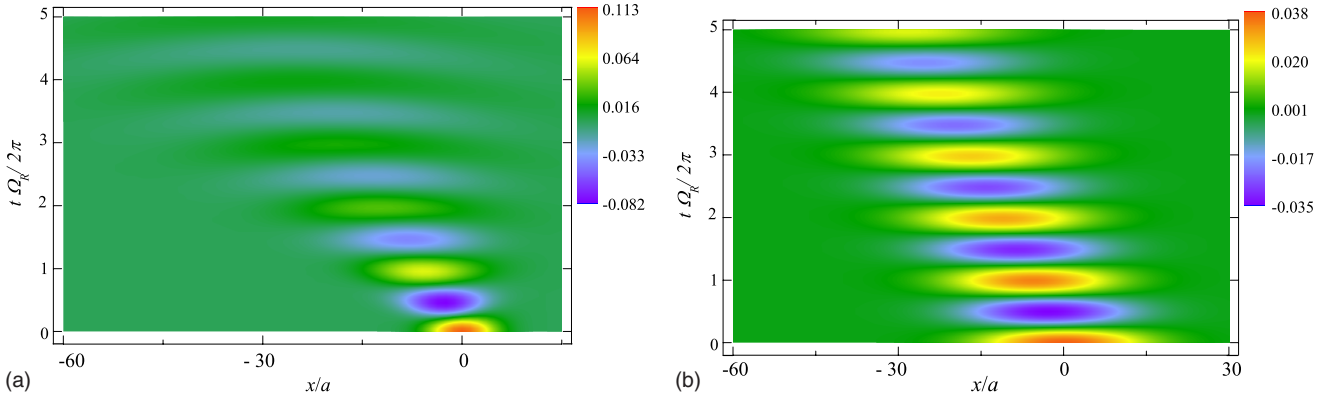

FIG. 11. (Color online) Space-time distribution of the inversion in the QD in the classical light chain for a single Gaussian wave packet $A(x,0)=(1/\sqrt[4]{\pi\sigma^2})\exp(-x^2/2\sigma^2)$, $B(x,0)=0$, $\xi_1=3\Omega_R$, $\xi_2=0.9\xi_1$, $\Delta=2(\xi_1-\xi_2)+\xi_2 a^2k^2$, $ka=0.33$, and $2\pi\lambda/\Omega_R=0.1$. (a) $\sigma=5a$ and (b) $\sigma=15a$.

$$|\Psi(t)\rangle=\sum_p (A_p(t)|a_p\rangle+B_p(t)|b_p\rangle), \tag{48}$$

where $A_p(t)$ and $B_p(t)$ are unknown functions. The equations of motion for them can now be obtained using approach of Sec. II B. Introducing the decay factor λ into the nonstationary Schrödinger equation and having made the continuous limit transition similar to the Sec. II C, we obtain the system of equations as follows:

$$\partial_t\mathbf{\Psi}=\left[2i\hat{\xi}-\frac{i\omega_0}{2}\hat{\sigma}_z-\frac{\lambda}{2}\hat{I}+\frac{i\Omega_R}{2}\hat{\kappa}(kx-\omega t)\right]\mathbf{\Psi}+ia^2\hat{\xi}\hat{\partial}_x^2\mathbf{\Psi}, \tag{49}$$

where $\mathbf{\Psi}(x,t)=\left[\begin{smallmatrix}A(x,t)\\B(x,t)\end{smallmatrix}\right]$. The system Eq. (49) may be considered as a particular case of the general system Eq. (11) and can be solved in the same way, which amounts to

$$\mathbf{\Psi}(x,t)=e^{i(kx-\omega t)\hat{\sigma}_z/2}e^{-\lambda t/2}\times\int_{-\infty}^{\infty}\hat{\rho}(h,t)\tilde{\mathbf{\Phi}}(h,0)e^{i\{hx+[\vartheta_1(h)+\vartheta_2(h)]t/2\}}dh. \tag{50}$$

Here, the values $\hat{\rho}(h,t)$, $\varphi^{\pm}(h,t)$, $\psi_h(t)$, $\delta_{\pm}(h)$, $\Omega(h)$, and $\Delta_{eff}(h)$ are determined by equalities in Eqs. (16), (17), (28), and (30)–(32), respectively, after implementing the replacement $2g\sqrt{n+1}\to\Omega_R$ therein [in doing so the photonic number dependence in $\hat{\rho}(h,t)$, $\varphi^{\pm}$, ψ_h, Ω disappears]. The vector function $\tilde{\mathbf{\Phi}}(h,0)$ is determined by the initial conditions similar to Eq. (33).

A typical space-time distribution of the inversion density $w(x,t)=a[|A(x,t)|^2-|B(x,t)|^2]$ is shown in Fig. 11. As is seen from the figure, the space-time dynamics of Rabi wave packet is similar to the case of vacuum oscillations but it is of substantially different physical nature: the reason of the QD quantum transition between excited and ground quantum states is the driving field action for quasiclassical case and spontaneous photon emission for vacuum oscillations. Note that more narrow wave packet spreads heavily, than the wider one [compare Figs. 11(a) and 11(b)].

Figure 12 illustrates the temporal behavior of the integral inversion for the case of classical light. Since the photon distribution does not change, collapses and revivals are absent. However, another phenomenon of the similar nature takes place because of distributive geometry of QD chain. In contrast to the isolated Rabi oscillator, the integral inversion in QD chain decreases as time increases. Such a damping is of nondissipative nature and keeps out even at $\lambda=0$. This trend can be explained in the following manner. The effective detuning $\Delta_{eff}(h)$ [and therefore the Rabi frequency $\Omega(h)$] depend on h, thereby implying that the Rabi-jump dynamics is presented as a superposition of harmonic oscillations with different frequencies. The existence of dephasing between different elementary oscillators leads to the damping of integral inversion similar to the effect of inhomogeneous broadening in the ensemble of nonidentical oscillators. The damping rate is controlled by the values of wave number k and coupling constants $\xi_{1,2}$. If the QD chain is initially prepared in the excited state $[B(x,0)=0]$, the damping is predominantly determined by the product $a\xi_2k$, while for the QD chain initially prepared in the ground state $[A(x,0)=0]$ it is entirely defined by $a\xi_1k$. In the case of coherent superposition as a initial state both $a\xi_1k$ and $a\xi_2k$ are important. If $k=0$, $\xi_1=\xi_2$, the dependence $\Delta_{eff}(h)$ and, respectively, the dephasing effect disappears. As a result, the integral inversion oscillates harmonically between −1 to 1 without damping (dotted curve in Fig. 12). In the weak cou-

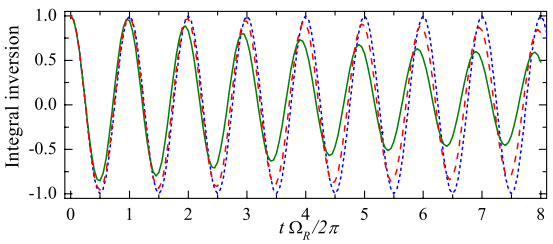

FIG. 12. (Color online) Temporal dependence of the integral inversion in the classical light for the input parameters as follows: $\Delta=0$, $k=0$, and $\xi_1=\xi_2=3\Omega_R$ (dotted line); $\Delta=\xi_2a^2k^2$, $ka=0.33$, and $\xi_1=\xi_2=3\Omega_R$ (solid line); and $\Delta=2(\xi_1-\xi_2)+\xi_2a^2k^2$, $ka=0.33$, $\xi_1=3\Omega_R$, and $\xi_2=1.5\Omega_R$ (dashed line). In all cases $\sigma=5a$ and $\lambda=0$.

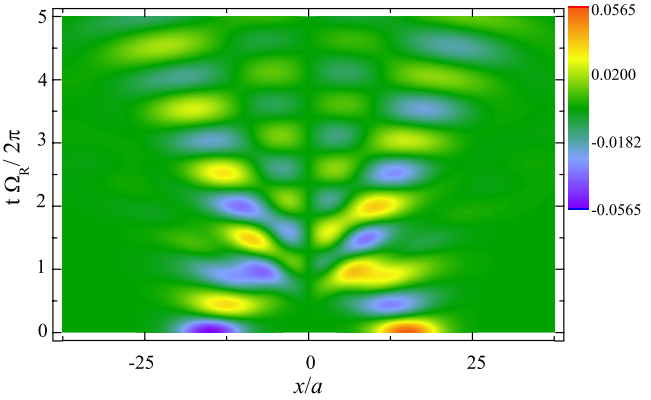

FIG. 13. (Color online) Space-time distribution of the inversion density in the QD chain in the classical light for two counterpropagating identical Gaussian wave packets: $A(x,0)=\exp[-(x-3\sigma)^2/2\sigma^2]/\sqrt[4]{4\pi\sigma^2}$, $B(x,0)=\exp[-(x+3\sigma)^2/2\sigma^2]/\sqrt[4]{4\pi\sigma^2}$, $\Delta=0$, $ka=0.33$, $\sigma=5a$, $\xi_1=\xi_2=3\Omega_R$, and $2\pi\lambda/\Omega_R=0.1$.

pling limit the indicated dephasing mechanism is analogous to the Landau damping in plasma.[50]

Interaction of two counterpropagating identical Gaussian Rabi wave packets colliding at $x=0$ is shown in Fig. 13. Unlike the case of quantum field, the space-time distribution of the inversion density is fully symmetrical with respect to the line $x=0$, and integral inversion does not oscillate at all: it is equal to zero for $t\geq 0$ and arbitrary values of Ω_R.

VI. INFLUENCE OF THE LOCAL-FIELD EFFECT

Local fields are depolarization fields arising inside QDs due to the dipole-dipole electron-hole interaction. As a result, the field acting on the e-h pair differs from mean field.[48] Hereafter this difference will be referred to as local-field effect. The local-field action is described by the component $\Delta\hat{H}$ of total Hamiltonian given by Eq. (4) and leads to a nonlinear terms in the equations of motion [last terms in Eqs. (6) and (7)]. The presence of nonlinearity results in the qualitatively new features of Rabi oscillations in single QDs.[17–19] The detailed analysis of the local-field influence on the Rabi waves is the subject for future investigations. In this section we consider only some aspects of this problem and give some simple estimations.

Let us consider finite (of the length L) QD chain interacting with classical light. The relaxation processes are neglected (i.e., $\lambda=0$). The equations of motion follow from Eqs. (6) and (7) in the same way as Eq. (11) reduces to Eq. (49) and have the form ($\xi_1=\xi_2=\xi$)

$$\partial_t A = -\frac{i}{2}(\omega_0 - 4\xi)A + \frac{i\Omega_R}{2}Be^{i(kx-\omega t)} + i\xi a^2\partial_x^2 A - i\Delta\omega|B|^2 A, \tag{51}$$

$$\partial_t B = \frac{i}{2}(\omega_0 + 4\xi)B + \frac{i\Omega_R}{2}Ae^{-i(kx-\omega t)} + i\xi a^2\partial_x^2 B - i\Delta\omega|A|^2 B. \tag{52}$$

Let us use the periodic boundary conditions (Born-von Karman conditions)

$$A(L/2,t) = A(-L/2,t), B(L/2,t) = B(-L/2,t). \tag{53}$$

Let us suppose that the electromagnetic field satisfies the periodic conditions Eq. (53), i.e., $kL=2\pi m$, where m is integer number. Let us seek partial solution of the system in Eqs. (51) and (52) in the form of traveling wave: $A(x,t)=u_0e^{i(h+k/2)x}e^{-i(\nu+\omega/2)t}$ and $B(x,t)=v_0e^{i(h-k/2)x}e^{-i(\nu-\omega/2)t}$, where u_0 and v_0 are the unknown constant amplitudes satisfying the normalization condition for wave function, h and ν are the unknown real values. Substituting A and B into Eqs. (51) and (52) we obtain

$$[\nu + \phi_1 - \Delta\omega|v_0|^2]u_0 + \frac{\Omega_R}{2}v_0 = 0, \tag{54}$$

$$[\nu + \phi_2 - \Delta\omega|u_0|^2]v_0 + \frac{\Omega_R}{2}u_0 = 0, \tag{55}$$

where $\phi_{1,2}(h)=2\xi_{1,2}\mp\Delta/2-\xi_{1,2}a^2(h\pm k/2)^2$. The use of boundary conditions Eq. (53) leads to a quantization condition for h: $h=\pi n/L$, n is integer. Expressing v_0 from Eq. (55) and substituting it into Eq. (54), we obtain

$$\nu + \phi_1(h) - \frac{\Omega_R^2[\nu + \phi_2(h)]}{4[\nu + \phi_2(h) - \Delta\omega|u_0|^2]^2} = 0. \tag{56}$$

The wave-function normalization condition amounts to

$$\left(1 + \frac{\Omega_R^2}{4|\nu + \phi_2(h) - \Delta\omega|u_0|^2|^2}\right)|u_0|^2 = \frac{1}{L}. \tag{57}$$

Equations (56) and (57) form the closed system of equations with respect to ν and $|u_0|^2$, which defines the spectrum of Rabi waves $\nu=\nu(h)=\nu(n)$ with regard to the local-field effect. It should be noted that only solutions with real-valued ν have physical meaning [otherwise the system Eqs. (54) and (55) contradicts to the initial Eqs. (51) and (52)]. In the limit cases $L\to\infty$ or $\Delta\omega\to 0$ the system [Eqs. (56) and (57)] reduces to the dispersion equation[45] for Rabi waves in the infinite QD chain interacting with classical light.

The spectrum of the Rabi waves for two essentially different values of L but identical $\Delta\omega$ and other parameters is shown in Fig. 14. The curves depicted in Fig. 14(a) correspond to the QD chain of large length. The local-field effect in this case is negligibly small, and the spectrum of the Rabi waves is practically identical to obtained in Ref. 45. For QD chain of the small length the situation becomes principally different due to the nonlinear effects. As a result, any cross point transforms to the *closed loop*, which corresponds to the appearance of two additional roots of system [Eqs. (56) and (57)]. Each of these roots corresponds to the existence of additional line in the Rabi wave spectrum. The size of this loop decreases as the ratio $\Delta\omega/\Omega_R$ decreases.

The detailed structure of the spectrum in the vicinity of the closed loop is shown in Fig. 14(c). Let us assume that the frequency of Rabi oscillations changes adiabatically (for example, due to the change in light frequency). Thus, the QD chain transverses to another spectral branch with otherwise

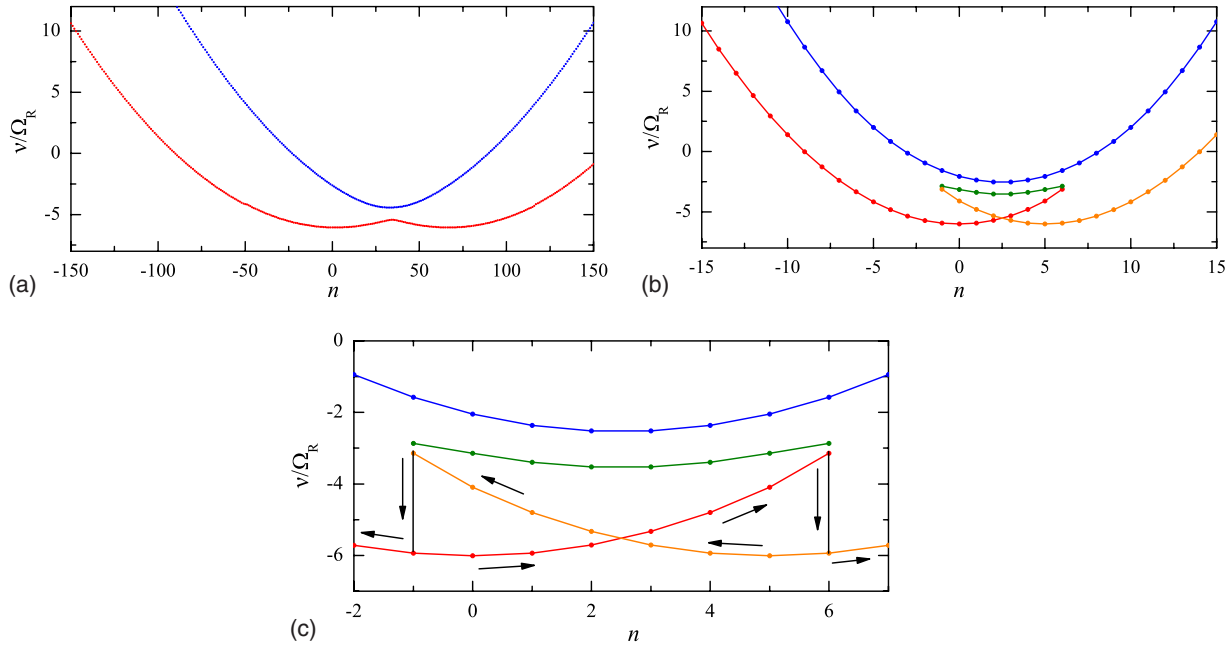

FIG. 14. (Color online) Dispersion curves for Rabi waves subject to local-field effects. (a) $L=200a$ and (b) and (c) $L=20a$. In all cases $\xi_1=\xi_2=3\Omega_R$, $ka=0.25\pi$, $\Delta=0$, and $\Delta\omega=100\Omega_R$. The discrete points, corresponding to different spectral lines, are joined together only to aid the eyes.

index n (and, correspondingly, wave number h). Such a set of transversions may be interpreted as an adiabatically slow movement of the quantum state of the QD chain in the ν-h plane [it is shown by the arrows in Fig. 14(c)]. The principal trend of such movement is the nonidentity of its trajectories for the opposite directions of motion. Thus, the loop is of hysteresis character, thereby the interaction of the local-field effect and Rabi waves leads to the bistability of quantum states in the QD chain. The detailed analysis of the stability of different spectral branches with respect to the infinitely small perturbations is the subject of future investigations.

Let us identify some sufficient conditions permitting us to neglect the local-field effect influence on the Rabi wave-propagation processes. An analysis in Ref. 19 for isolated QD has shown that the local-field effect can work on the Rabi oscillations in two different regimes, which are caused by the relation between Rabi oscillation frequency $\Omega_{\langle n\rangle}=\sqrt{\Delta^2+4g^2(\langle n\rangle+1)}$, ($\langle n\rangle$ is the average photon number) and depolarization shift $\Delta\omega$. In the first regime, established by the condition $\Omega_{\langle n\rangle}\gtrsim\Delta\omega$, local-field effect very slightly affects the Rabi dynamics. As a result, the integral inversion oscillates between -1 and 1, and ordinary physical picture of collapses and revivals takes place. In the second regime dictated by the opposite condition $\Omega_{\langle n\rangle}<\Delta\omega$, time evolution of inversion is strongly affected by the local-field effect. In contrast, integral inversion oscillates between -1 and 0, and the collapse-revivals effect completely disappears (for details see Ref. 19). The role of $\Omega_{\langle n\rangle}$ for QD chain is played by the difference $\nu_1(n,h)-\nu_2(n,h)$, determined by Eq. (15), whereby we conclude that the local field omitting for traveling wave is justified in the first regime, wherein the condition

$$\nu_1(n,h)-\nu_2(n,h)\gtrsim\Delta\omega, \tag{58}$$

holds true. In the case of Rabi wave packet the local field neglecting permissible if the condition in Eq. (58) hold in the vicinity of the localization points of spatial spectrum, i.e., $\nu_1(\langle n\rangle,h_{1,2}^{(0)})-\nu_2(\langle n\rangle,h_{1,2}^{(0)})\gtrsim\Delta\omega$, while in the second regime, wherein the condition in Eq. (58) breaks down, a more rigorous analysis based on the system Eqs. (6) and (7) is required.

VII. CORRELATION FUNCTIONS

Whereas Secs. IV–VI address the inversion density and integral inversion, we now proceed to the exciton-exciton and exciton-photon multitime correlation functions of the Rabi waves. For this purpose it is convenient to use the initial discrete model of QD chain and make the transition to the continuous limit only on the final step of analysis. Along with the Schrödinger picture operators $\hat{\sigma}_p^{\pm}$, we introduce the Heisenberg picture operators $\hat{\sigma}_p^{\pm}(t)$ presented in the terms of evolution operator $\hat{U}(t,0)$ as $\hat{\sigma}_p^{\pm}(t)=\hat{U}^{+}(t,0)\hat{\sigma}_p^{\pm}\hat{U}(t,0)$. Omitting intermediate steps provided in appendix, we present here only the final result for evolution operator

$$\hat{U}(t,0)=\frac{a}{2\pi}\sum_n\sum_{p,q}\int_{-\pi/a}^{\pi/a}\{\varphi_n^{-}(h,t)e^{i\delta_h^{+}t}|a_p,n\rangle\langle a_q,n|+\psi_n(h,t)\times[e^{i\delta_h^{+}t}|a_p,n\rangle\langle b_q,n+1|+e^{i\delta_h^{-}t}|b_p,n+1\rangle\langle a_q,n|]+\varphi_n^{+}(h,t)e^{i\delta_h^{-}t}|b_p,n+1\rangle\langle b_q,n+1|\}e^{ih(p-q)a}dh. \tag{59}$$

Here $\varphi_n^{\pm}(h,t)$, $\psi_n(h,t)$, and $\Omega_n(h)$ are given by formulas (16), (30), and (31), respectively. Quantities $\delta_h^{\pm}$ and $\Delta_{eff}(h)$ are defined by expressions (17) and (32) after implementing the replacements $\vartheta_{1,2}\to 2\xi_{1,2}\cos[(h\pm k/2)a]$.

According to Eq. (59) the exciton-exciton correlation functions $G_{p,q}^{(1)}(t,t')\equiv\langle\hat{\sigma}_p^{+}(t)\hat{\sigma}_q^{-}(t')\rangle$ can be represented as follows:

$$G_{p,q}^{(1)}(t,t') = \frac{a^4}{16\pi^4}\sum_n \sum_{l,r} \int\int\int_{-\pi/a}^{\pi/a} e^{ih'(p-q)a} e^{i(qg-ph)a} e^{i(lh-rg)a} e^{-i\Delta(t-t')} [\varphi_n^+(h',t)\varphi_n^-(h',t')$$
$$\times -\psi_n(h',t)\psi_n(h',t')][\varphi_{n+1}^+(h,t)\varphi_{n+1}^-(g,t')u_{l,n+1}^*(0)u_{r,n+1}(0)$$
$$\times +\psi_{n+1}(h,t)\psi_{n+1}(g,t')v_{l,n+2}^*(0)v_{r,n+2}(0) + \varphi_{n+1}^+(h,t)\psi_{n+1}(g,t')u_{l,n+1}^*(0)v_{r,n+2}(0)$$
$$\times -\psi_{n+1}(h,t)\varphi_{n+1}^-(g,t')v_{l,n+2}^*(0)u_{r,n+1}(0)]dh'dhdg, \tag{60}$$

where $u_{p,n}(t)=A_{p,n}(t)e^{-i(kpa-\omega_0 t)/2}$ and $v_{p,n+1}(t)=B_{p,n+1}(t)e^{i(kpa-\omega_0 t)/2}$.

One can see that in general case $G_{p,q}^{(1)}(t,t')$ cannot be represented as $G_{p-q}^{(1)}(t,t')$ or $G_{p,q}^{(1)}(t-t')$. It indicates the absence both spatial and time homogeneity.

Let us consider the case of $B_{p,n+1}(0)=0$ and $t'=0$. Then taking into account that $\psi_n(h,0)=0$, $\varphi_n^{\pm}(h,0)=1$, and $\int_{-\pi/a}^{\pi/a} e^{ig(q-r)a}dg = 2\pi\delta_{qr}/a$, we obtain rather simple expression for correlation function

$$G_{p,q}^{(1)}(t,0) = \frac{a^3 e^{-i\Delta t}}{8\pi^3}\sum_n \sum_l \int\int_{-\pi/a}^{\pi/a} e^{ih'(p-q)a} e^{ih(l-p)a} \varphi_n^+(h',t)\varphi_{n+1}^+(h,t)u_{l,n+1}^*(0)u_{q,n+1}(0)dh'dh. \tag{61}$$

Having made the substitutions $pa\to x$, $qa\to x'$, $\Sigma_l \to \frac{1}{a}\int_{-\infty}^{\infty}\ldots dz$, $\Sigma_r \to \frac{1}{a}\int_{-\infty}^{\infty}\ldots dz'$ and approximation $\cos[(h\pm k/2)a]\cong 1-(h\pm k/2)^2a^2/2$, we obtain the corresponding correlation function in the continuous limit as

$$G^{(1)}(x,x',t,0) = \frac{a^2 e^{-i\Delta t}}{8\pi^3}\sum_n \int_{-\infty}^{\infty}\int\int_{-\pi/a}^{\pi/a} e^{ih'(x-x')} e^{ih(z-x)} \varphi_n^+(h',t)\varphi_{n+1}^+(h,t)u_{n+1}^*(z,0)u_{n+1}(x',0)dh'dhdz. \tag{62}$$

The plot of normalized correlation function

$$g^{(1)}(x,x',t,t') = \frac{G^{(1)}(x,x',t,t')}{\sqrt{G^{(1)}(x,x,0,0)G^{(1)}(x',x',0,0)}} \tag{63}$$

for $x'=0$, $t'=0$ is presented on Fig. 15. The external electromagnetic field and electron in the QD chain are supposed to be initially in a single number state and excited state $[B_{n+1}(x,0)=0]$, respectively.

The correlation function of the polarization operator $\hat{\sigma}_p^+(t)$ with the operator of the external field $\hat{E}_p^-(t)=\mathcal{E}\hat{a}e^{i(kpa-\omega t)}$ (exciton-photon correlators) appears as

$$\langle \hat{E}_q^-(t')\hat{\sigma}_p^+(t)\rangle = \frac{a^2\mathcal{E}}{4\pi^2}\sum_n \sum_{l,r} \int\int_{-\pi/a}^{\pi/a} dhdh'\{\varphi_{n+1}^+(h',t)\sqrt{n+1}[\psi_n(h,t)u_{r,n}^*(0)u_{l,n}(0) + \varphi_n^+(h,t)u_{r,n}^*(0)v_{l,n+1}(0)]$$
$$-\psi_{n+1}(h',t)\sqrt{n+2}[\psi_n(h,t)v_{r,n+1}^*(0)u_{l,n}(0) + \phi_n^+(h,t)v_{r,n+1}^*(0)v_{l,n+1}(0)]\}e^{ipa(h-h')}e^{i(h'r-hl)a}e^{i(kpa-\omega_0 t)}e^{i\omega(t-t')}. \tag{64}$$

VIII. CONCLUSION

To conclude, we have developed a theory of Rabi oscillations in a periodical 1D chain of two-level QDs with tunneling coupling, exposed to quantum light. The influence of interdot coupling and Rabi oscillations on each other was considered in detail. The following conclusions are emerged from our studies. (i) The interdot tunneling in the QD chain exposed to quantum light leads to the appearance of spatial modulation of Rabi oscillations (Rabi waves propagation). Calculated data indicate that Rabi waves can propagate if the light mode wave vector has nonzero component along the chain axis. Characteristics of the Rabi waves depend strongly on relations between parameter of electron-photon coupling, frequency deviation and transparency factors of potential barriers for both of levels.

(ii) Traveling Rabi wave represent the quantum state of QD chain dressed by radiation, i.e., entangled states of e-h pair and photons. The qualitative distinction of these states from the similar states of single dressed atom[2] is the space-time modulation of dressing parameter according to the traveling wave law. The propagation of traveling Rabi wave looks like supported by periodically inhomogeneous nonreciprocal effective media, whose refractive index is deter-

mined by electric field distribution. This states can be treated as a quasiparticles of a new type (it may be considered as a generalization of Hopfield polaritons[51,53] for the case of indirect quantum transitions).

(iii) Two traveling Rabi modes with different frequencies of Rabi oscillations exist at a given value of wave number. The range of Rabi oscillation frequencies is limited by the critical value, different for both of the modes. The QD chain is opaque in the regime of Rabi oscillation frequencies below the critical value. The critical frequencies and dispersion characteristics of Rabi modes depend on number of photons.

(iv) Different types of Rabi wave packets are formed as an arbitrary superpositions of four partial subpackets with different amplitudes, frequency shifts, and velocities of motion. Two of subpackets correspond to the contribution of excited initial state and two others caused by the ground initial state contribution. Rabi wave packets transfer energy, inversion, quasimomentum, electron-electron, and electron-photon quantum correlations along the chain. The number of subpackets can be diminished in specific circumstances.

(v) Rabi oscillations qualitatively change the electron tunneling picture in the QD chain. In contrast to the absence of electron-photon coupling, the movement of initially ground-state subpacket is governed by tunneling transparency of excited energy level and vice versa. Thus, Rabi oscillations can stimulate the tunneling through low-energy level and suppress it through high-energy one.

(vi) Rabi wave packet movement along the QD chain alters the light statistics. Particularly, for the QD chain, exposed to coherent light, we predict the drastic modification of the standard collapse-revival phenomenon: collapses and revivals due to the interdot tunneling appear in different areas of space.

Rabi waves can take place in a number of other distributed systems strongly coupled with electromagnetic field. The example is superconducting circuits based on Josephson junctions, which are currently the most experimentally advanced solid-state qubits.[10] It is evident, for example, that the qubit-qubit capacitance coupling in the chain of qubits placed inside a high-Q transmission-line resonator will be responsible for the Rabi waves propagation similar to described in this paper.

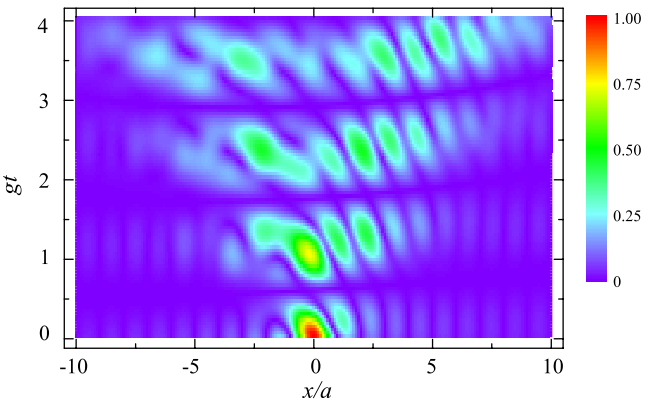

FIG. 15. (Color online) The space-time dependence of normalized correlation function $g^{(1)}(x,0,t,0)$ for light in Fock state with $n=5$ and the input parameters as follows: $\xi_1=\xi_2=10g$, $\Delta=\xi_2 k^2a^2$, $\sigma=5a$, $A_n(x,0)=\exp(-x^2/2\sigma^2)/\sqrt[4]{\pi\sigma^2}$, and $B_{n+1}(x,0)=0$.

ACKNOWLEDGMENTS

The work of G. Ya. Slepyan was partially carried out during the stay at the Institut für Festkörperphysik, TU Berlin, and supported by the Deutsche Forschungsgemeinschaft (DFG). Authors are grateful to S. A. Maksimenko, D. S. Mogilevtsev, J. Haverkort, and A. M. Nemilentsau for stimulative discussions.

APPENDIX: EVOLUTION OPERATOR

The wave function at time t in terms of the wave function at time $t=0$ is given by $|\Psi(t)\rangle=\hat{U}(t,0)|\Psi(0)\rangle$, where $\hat{U}(t,0)$ is the evolution operator. The task of this appendix is the calculation of the evolution operator for a discrete QD chain exposed to quantum light. The outcome of appendix is Eq. (59), which allows to pass from Schrödinger picture to the Heisenberg one and would be used in the calculations of different types of correlators. Let us for simplicity omit the dissipation, thus, the evolution operator is unitary.

Let us introduce new variables $u_{p,n}=A_{p,n}e^{-i(kpa-\omega_0 t)/2}$ and $v_{p,n+1}=B_{p,n+1}e^{i(kpa-\omega_0 t)/2}$. It then follows from Eqs. (6) and (7) that

$$\partial_t u_{p,n}=i\xi_1(u_{p-1,n}e^{-ika/2}+u_{p+1,n}e^{ika/2})-ig\sqrt{n+1}v_{p,n+1}e^{i\Delta t}, \tag{A1}$$

$$\partial_t v_{p,n+1}=i\xi_2(v_{p-1,n+1}e^{ika/2}+v_{p+1,n+1}e^{-ika/2})-ig\sqrt{n+1}u_{p,n}e^{-i\Delta t}. \tag{A2}$$

Coefficients in this system do not depend from QD number p. It allows us to seek the solution in the form of traveling wave: $u_{p\pm1,n}=u_{p,n}e^{\pm iha}$, $v_{p\pm1,n+1}=v_{p,n+1}e^{\pm iha}$, and $ha\in[-\pi,\pi]$. Then the pairs of equations for different QDs become independent of each other and may be written as

$$\partial_t u_{p,n}=2i\xi_1\cos[(h+k/2)a]u_{p,n}-ig\sqrt{n+1}v_{p,n+1}e^{i\Delta t}, \tag{A3}$$

$$\partial_t v_{p,n+1}=2i\xi_2\cos[(h-k/2)a]v_{p,n+1}-ig\sqrt{n+1}u_{p,n}e^{-i\Delta t}. \tag{A4}$$

The initial conditions can be presented as $u_{p,n}(0)=a_n e^{ihpa}$ and $v_{p,n+1}(0)=b_{n+1}e^{ihpa}$, where a_n and b_n are given numbers satisfying the normalization condition for wave function. The system Eqs. (A3) and (A4) can be easily integrated, the result is given by

$$u_{p,n}(t)=C_1^n(0)e^{i[\delta_h^+-\Omega_n(h)/2]t}+C_2^n(0)e^{i[\delta_h^++\Omega_n(h)/2]t}, \tag{A5}$$

where $C_{1,2}^n(0)$ are constants of integration which are determined from the initial conditions. Writing the latter in the form $u_{p,n}(0)=a_n e^{ihpa}$ and $v_{p,n+1}(0)=b_{n+1}e^{ihpa}$, we then have

$$u_{p,n}(t)=[\alpha_n e^{i[\delta_h^+-\Omega_n(h)/2]t}+\beta_n e^{i[\delta_h^++\Omega_n(h)/2]t}]e^{ihpa} \tag{A6}$$

and

$$v_{p,n+1}(t)=[\gamma_n e^{i[\delta_h^--\Omega_n(h)/2]t}+\delta_n e^{i[\delta_h^-+\Omega_n(h)/2]t}]e^{ihpa}, \tag{A7}$$

where $\delta_h^\pm=\xi_1\cos[(h+k/2)a]+\xi_2\cos[(h-k/2)a]\pm\Delta/2$ and

$$\alpha_n = \frac{\Omega_n(h) + \Delta_h}{2\Omega_n(h)} a_n + \frac{g\sqrt{n+1}}{\Omega_n(h)} b_{n+1}, \tag{A8}$$

$$\beta_n = \frac{\Omega_n(h) - \Delta_h}{2\Omega_n(h)} a_n - \frac{g\sqrt{n+1}}{\Omega_n(h)} b_{n+1}, \tag{A9}$$

$$\gamma_n = \frac{g\sqrt{n+1}}{\Omega_n(h)} a_n + \frac{\Omega_n(h) - \Delta_h}{2\Omega_n(h)} b_{n+1}, \tag{A10}$$

$$\delta_n = -\frac{g\sqrt{n+1}}{\Omega_n(h)} a_n + \frac{\Omega_n(h) + \Delta_h}{2\Omega_n(h)} b_{n+1}. \tag{A11}$$

Basis wave function has the form

$$|\Psi_h(t)\rangle = \sum_n \sum_p \left(u_{p,n}(t)|a_p, n\rangle + v_{p,n+1}(t)|b_p, n+1\rangle\right). \tag{A12}$$

We now can represent the required wave function as Fourier integral with basis functions $\Psi_h(t)$

$$|\Psi(t)\rangle = \int_{-\pi/a}^{\pi/a} M(h)|\Psi_h(t)\rangle dh, \tag{A13}$$

where $M(h)$ is unknown weighting function. To express it let us take into account, that

$$|\Psi(0)\rangle = \sum_{n,p} \int_{-\pi/a}^{\pi/a} M(h)[a_n|a_p, n\rangle + b_{n+1}|b_p, n+1\rangle] e^{ihpa} dh, \tag{A14}$$

where

$$\langle a_p, n|\Psi(0)\rangle = a_n \int_{-\pi/a}^{\pi/a} M(h) e^{ihpa} dh \tag{A15}$$

and the same for $\langle b_p, n+1|\Psi(0)\rangle$. Then employing inverse Fourier transform we have

$$a_n M(h) = \frac{a}{2\pi} \sum_{q=-\infty}^{\infty} \langle a_q, n|\Psi(0)\rangle e^{-ihqa} \tag{A16}$$

and analogously for b_{n+1}.

Substituting Eq. (A16) into Eq. (A13), we obtain Eq. (59).

*jarchak@gmail.com

[1] M. O. Scully and M. S. Zubairy, *Quantum Optics* (Cambridge University Press, Cambridge, 2001).

[2] C. Cohen-Tannoudji, J. Dupont-Roc, and G. Grynberg, *Atom-Photon Interactions: Basis Properties and Applications* (Wiley, Chichester, 1998).

[3] I. I. Rabi, Phys. Rev. **51**, 652 (1937).

[4] H. C. Torrey, Phys. Rev. **76**, 1059 (1949).

[5] G. B. Hocker and C. L. Tang, Phys. Rev. Lett. **21**, 591 (1968).

[6] T. A. Johnson, E. Urban, T. Henage, L. Isenhower, D. D. Yavuz, T. G. Walker, and M. Saffman, Phys. Rev. Lett. **100**, 113003 (2008).

[7] H. Kamada, H. Gotoh, J. Temmyo, T. Takagahara, and H. Ando, Phys. Rev. Lett. **87**, 246401 (2001).

[8] A. Blais, R.-S. Huang, A. Wallraff, S. M. Girvin, and R. J. Schoelkopf, Phys. Rev. A **69**, 062320 (2004).

[9] J. Gambetta, A. Blais, D. I. Schuster, A. Wallraff, L. Frunzio, J. Majer, M. H. Devoret, S. M. Girvin, and R. J. Schoelkopf, Phys. Rev. A **74**, 042318 (2006).

[10] A. Blais, J. Gambetta, A. Wallraff, D. I. Schuster, S. M. Girvin, M. H. Devoret, and R. J. Schoelkopf, Phys. Rev. A **75**, 032329 (2007).

[11] G. Burkard and A. Imamoglu, Phys. Rev. B **74**, 041307(R) (2006).

[12] S. D. Barrett and G. J. Milburn, Phys. Rev. B **68**, 155307 (2003).

[13] C. K. Law and J. H. Eberly, Phys. Rev. Lett. **76**, 1055 (1996).

[14] Y. Yang, J. Xu, G. Li, and H. Chen, Phys. Rev. A **69**, 053406 (2004).

[15] J. Förstner, C. Weber, J. Danckwerts, and A. Knorr, Phys. Rev. Lett. **91**, 127401 (2003).

[16] A. Vagov, M. D. Croitoru, V. M. Axt, T. Kuhn, and F. M. Peeters, Phys. Rev. Lett. **98**, 227403 (2007).

[17] G. Ya. Slepyan, A. Magyarov, S. A. Maksimenko, A. Hoffmann, and D. Bimberg, Phys. Rev. B **70**, 045320 (2004).

[18] E. Paspalakis, A. Kalini, and A. F. Terzis, Phys. Rev. B **73**, 073305 (2006).

[19] G. Ya. Slepyan, A. Magyarov, S. A. Maksimenko, and A. Hoffmann, Phys. Rev. B **76**, 195328 (2007).

[20] O. V. Kibis, G. Ya. Slepyan, S. A. Maksimenko, and A. Hoffmann, Phys. Rev. Lett. **102**, 023601 (2009).

[21] Th. Unold, K. Mueller, C. Lienau, Th. Elsaesser, and A. D. Wieck, Phys. Rev. Lett. **94**, 137404 (2005).

[22] J. Gea-Banacloche, M. Mumba, and M. Xiao, Phys. Rev. B **74**, 165330 (2006).

[23] L. Saelen, R. Nepstad, I. Degani, and J. P. Hansen, Phys. Rev. Lett. **100**, 046805 (2008).

[24] S. Hughes, Phys. Rev. Lett. **94**, 227402 (2005).

[25] J. Danckwerts, K. J. Ahn, J. Förstner, and A. Knorr, Phys. Rev. B **73**, 165318 (2006).

[26] Ho Trung Dung, L. Knöll, and D.-G. Welsch, Phys. Rev. A **66**, 063810 (2002).

[27] A. V. Tsukanov, Phys. Rev. B **73**, 085308 (2006).

[28] Y. R. Shen, *The Principles of Nonlinear Optics* (Wiley, New York, 1984).

[29] I. Waldmueller, W. W. Chow, and A. Knorr, Phys. Rev. B **73**, 035433 (2006).

[30] F. Le Kien and K. Hakuta, Phys. Rev. A **77**, 033826 (2008).

[31] T. S. Tsoi and C. K. Law, Phys. Rev. A **78**, 063832 (2008).

[32] L. Allen and J. H. Eberly, *Optical Resonance and Two-Level Atoms* (Dover, New York, 1975).

[33] R. Loudon, *The Quantum Theory of Light* (Clarendon, Oxford, 1983).

[34] M. Wubs, L. G. Suttorp, and A. Lagendijk, Phys. Rev. A **70**, 053823 (2004).

[35] M. W. Sorensen and A. S. Sorensen, Phys. Rev. A **77**, 013826 (2008).
[36] G. Ya. Slepyan, S. A. Maksimenko, A. Lakhtakia, O. Yevtushenko, and A. V. Gusakov, Phys. Rev. B **60**, 17136 (1999).
[37] L. Novotny and B. Hecht, *Principles of Nano-Optics* (Cambridge University Press, Cambridge, 2006).
[38] M. Tavis and F. W. Cummings, Phys. Rev. **170**, 379 (1968).
[39] In Hamiltonian $\hat{H}_f$ the constant term describing the photon vacuum contribution is omitted. In single-mode assumption its influence identically equal to zero. In so doing we are not interested in effects of spontaneous decay and Lamb shift. These effects are caused by interaction of the system with photon vacuum and can be taken into account in multimode assumption only.
[40] Ph. A. Martin and F. Rothen, *Many-Body Problems and Quantum Field Theory* (Springer-Verlag, Berlin, 2002).
[41] J. P. Reithmaier, G. Sek, A. Löffler, C. Hofmann, S. Kuhn, S. Reitzenstein, L. V. Keldysh, V. D. Kulakovskii, T. L. Reinecke, and A. Forchel, Nature (London) **432**, 197 (2004).
[42] H. J. Krenner, M. Sabathil, E. C. Clark, A. Kress, D. Schuh, M. Bichler, G. Abstreiter, and J. J. Finley, Phys. Rev. Lett. **94**, 057402 (2005).
[43] L. A. Openov, Phys. Rev. B **60**, 8798 (1999).
[44] M. F. Doty, J. I. Climente, M. Korkusinski, M. Scheibner, A. S. Bracker, P. Hawrylak, and D. Gammon, Phys. Rev. Lett. **102**, 047401 (2009).
[45] G. Ya. Slepyan, Y. D. Yerchak, S. A. Maksimenko, and A. Hoffmann, Phys. Lett. A **373**, 1374 (2009).
[46] P. Borri, W. Langbein, U. Woggon, V. Stavarache, D. Reuter, and A. D. Wieck, Phys. Rev. B **71**, 115328 (2005).
[47] S. Stufler, P. Ester, A. Zrenner, and M. Bichler, Phys. Rev. B **72**, 121301(R) (2005).
[48] G. Ya. Slepyan, S. A. Maksimenko, A. Hoffmann, and D. Bimberg, Phys. Rev. A **66**, 063804 (2002).
[49] A. Nazir, B. W. Lovett, S. D. Barrett, J. H. Reina, and G. A. D. Briggs, Phys. Rev. B **71**, 045334 (2005).
[50] E. M. Lifshitz and L. P. Pitaevskii, *Physical Kinetics* (Pergamon, Oxford, 1981).
[51] A. Kavokin, J. J. Baumberg, G. Malpuech, and F. P. Laussy, *Microcavities* (Oxford University Press, New York, 2007).
[52] S. M. Dutra, *Cavity Quantum Electrodynamics: The Strange Theory of Light in a Box* (Wiley Interscience, Hoboken, 2005).
[53] J. J. Hopfield, Phys. Rev. **112**, 1555 (1958).
[54] A. Quattropani, L. C. Andreani, and F. Bassani, Nuovo Cimento Soc. Ital. Fis. **7D**, 55 (1986).
[55] Two stationary states exist for two-level system exposed to classical light. These states correspond to the initial condition $A(0)=\Theta/\sqrt{1+\Theta^2}$ and $B(0)=1/\sqrt{1+\Theta^2}$, where $\Theta=\Omega_R/(\Delta\pm\sqrt{\Delta^2+\Omega_R^2})$, and characterized by constant in time-inversion numbers $w=\mp\Delta/\sqrt{\Delta^2+\Omega_R^2}$.
[56] J. H. Eberly, N. B. Narozhny, and J. J. Sanchez-Mondragon, Phys. Rev. Lett. **44**, 1323 (1980).